CHAPTER 3

Results and Discussion

A gas chromatograph with nitrogen phosphorous detector (GC-NPD) was used for the determination of dimethylamine (DMA) and trimethylamine (TMA) in fish and shrimp samples using a 25 m × 0.32 mm i.d. × 0.52 μm film thickness fused silica HP-FFAP capillary column consists of nitroterephthalic acid modified polyethylene glycol. A laboratory-built stainless steel water bath with a control heating coil and stainless steel adapter for vial holder was used for the headspace system.

3.1 Optimization of the GC-NPD conditions for DMA and TMA analysis

3.1.1 Carrier gas flow rate

Carrier gas (helium, He) flow rate was optimized in experiment 2.6.1 by considering the relationship between the height equivalent to a theoretical plate (HETP) and the carrier gas flow rate. HETP can be calculated by the van Deemter equation (equation 3.1) (Grob, 2004).

$$\text{HETP} = A + \frac{B}{u} + Cu \qquad (3.1)$$

Where A is eddy diffusion term that the mobile phase diffused through the particles of packing in the column. The result is shown in the velocity of mobile phase.

B is longitudinal or ordinary diffusion term resulted from the movement of molecules after collision in the column.

C is resistant to mass transfer term that a constant amount of the mass transfer.

The van Deemter equation shows the effect of the change in linear gas velocity on HETP. This equation represents a hyperbola that has a minimum velocity, at $u = (B/C)^{1/2}$ and a minimum HETP value (HETP_{min}) at $A+2(BC)^{1/2}$. The constants

can be calculated from an experimental plot of HETP *versus* linear gas velocity (Grob, 2004) as shown in Figure 3.1.

The first term, eddy diffusion (A term) accounts for the geometry of the packing. This term describes the change in pathway and velocity of solute molecules in reference to the zone center. Therefore, when a sample migrates down the column, each molecule has different paths and each path is of a different length. Some molecules take the longer paths and other take the shorter paths. There are also variations in the velocities of the mobile phase within these pathways. The overall result is that some molecules lag behind the center of the zone, whereas others move ahead of the zone. Therefore, the eddy diffusion process results in flow along randomly space variable-size particles in the column. Eddy diffusion term was quantified from the equation $A = 2\lambda d_p$, λ is a constant characteristic of packing and d_p is a diameter particle of packing. The contribution of the $2\lambda d_p$ term can be decreased by reducing the particle size (Grob, 2004).

The second term, B/u, describes the longitudinal diffusion term, $B = 2\lambda d_g/u$, d_g is the diffusion coefficients of the component in gas phase. This term is a measure of effect of molecular diffusion on zone spreading. If the velocity of the mobile phase is high then the analyte spends less time on the column, with decreases the effects of longitudinal diffusion. The optimum velocity is greatest for column packed with small particles and for mobile phase in which the solutes have a high diffusivity gas of low density, *e.g.*, hydrogen or helium (Grob, 2004).

The final term, C is the resistant to mass transfer term that a constant amount of the mass transfer. $C = (8/\pi^2)[k+(1+k)^2](d_f^2/D_l)$ where k is retention factor (capacity factor), d_f is effective film thickness of liquid phase and D_l is diffusivity of solute in liquid phase (Grob, 2004). An obvious way of reducing this term is to reduce the liquid film thickness. This causes a reduction in k and an increase in the term $k/(1+k)^2$ the k term is temperature dependent, so we can increase k and decrease $k/(1+k)^2$ by lowering the temperature. Lowering the temperature increase viscosity and thus decrease D_l. Therefore, the effect of factor $k/(1+k)^2$ and $1/D_l$ counteract each other. This term can be represented as the composite of the resistance to mass transfer in the mobile phase C_g and that in

the stationary phase C_l: $C = C_g + C_l$ the C term accounts for resistance to mass transfer in the liquid phase (Grob, 2004).

From equation (3.1), at low u, the B term is large, but quickly diminishes with increasing u and C_g to a lesser extent, C_l, then dominates. The smallest value of HETP is $HETP_{min}$, at with u is optimum, u_{opt}. The greater u_{opt}, the faster a sample can be analysed (Baugh, 1993).

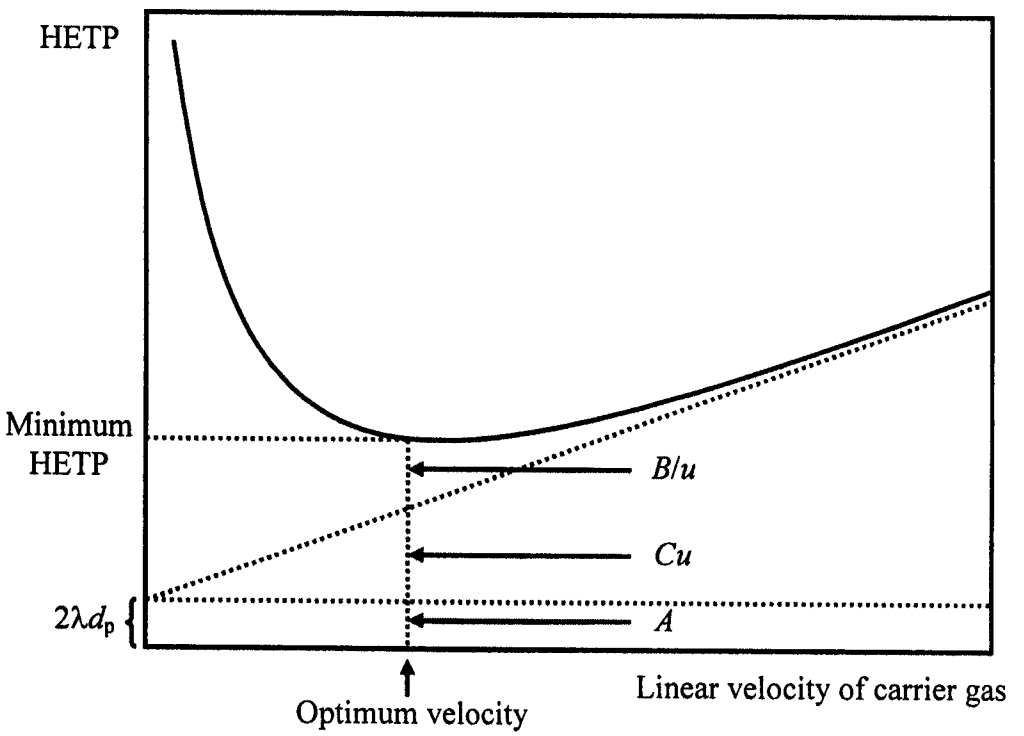

Figure 3.1 The van Deemter plot

In this research, 25 m × 0.32 mm i.d. narrow bore wall-coated open tubular (WCOT) capillary column was used for the analysis. A capillary column is a fused-silica tube of very small internal diameter (generally between 0.20-0.53 mm). The inner surface of a capillary column is coated with a thin layer of stationary phase so it is still possible for the solute molecules to come in contact with the inner walls of the tubing. In this column a liquid phase is coated on fused-silica wall with no packing material, therefore, the A term (eddy diffusion) is nonexistent because there is only one flow path and no packing material. The resistance to mass transfer term C

has the greatest effect on band broadening, and its effect in capillary columns is controlled by the mass transfer in the gas phase C_g. Thus, equation (3.1) takes a different form for capillary column, and this known as the Golay equation (Grob, 2004) in equation (3.2).

$$\text{HETP} = B/u + C_g u \tag{3.2}$$

The above equation showed that HETP is proportional to the flow rate of carrier gas (u). It is also known that an optimum carrier gas flow rate will give an optimum column resolution with the narrowest HETP (Grob, 2004).

In practical, the terms of A, B and C in the equation (3.1), are difficult to obtain. However, the plate theory assumes that the column is divided into a number of zones called *theoretical plate* (N). The zone thickness or height equivalent to a theoretical plate (HETP) is determined by assuming that there is perfect equilibrium between the gas and liquid phases within each plate. The indication of column efficiency in the term of HETP is determined by equation (3.3)

$$\text{HETP} = \frac{L}{N} \tag{3.3}$$

where L is length of column in centimeters

N is the number of theoretical plates

The plate number, N, of a column can be calculate from equation (3.4)

$$N = 16\left(\frac{t_R}{w}\right)^2 \tag{3.4}$$

where t_R is the retention time of the peak, w is the base peak width. If a width at half height ($w_{1/2}$) was used instead of a width (w) at the base, the plate number could be calculated by equation (3.5) (Tibor and Esther, 1999) (Figure 3.2)

$$N = 5.54\left(\frac{t_R}{w_{1/2}}\right)^2 \qquad (3.5).$$

Since a capillary column was used in this work, the plate number N could be calculated directly from the value obtained from a chromatogram as shown in the Figure 3.2 and equation 3.6 (Grob, 2004)

$$N = 2\pi(t_R h / A)^2 \qquad (3.6)$$

Where A is integrated peak area

h is integrated peak height

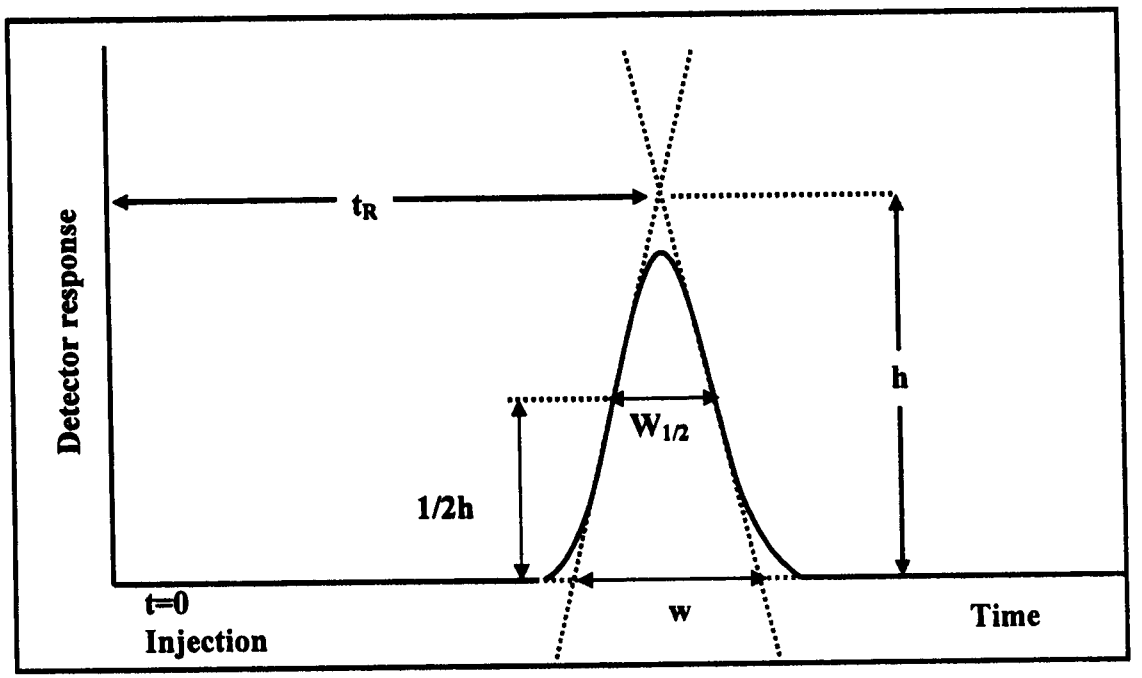

Figure 3.2 Measurement used in calculating total theoretical plates

N was calculated by equation 3.6 and substituted in equation 3.3 with a known L (column length) to obtain HETP. The values of HETP obtained at different carrier gas flow rate are shown in Table 3.1 and Figure 3.3. From the van Deemter

plot, the optimum flow rate of 3.0 mL min^{-1} for both DMA and TMA was obtained at the narrowest HETP and this provided the highest column efficiency.

Table 3.1 HETP of DMA (100 μg mL^{-1}) and TMA (1 μg mL^{-1}) standard solution at various carrier gas flow rates

Flow rate (mL min^{-1})	HETP (cm)*	
	DMA	TMA
2.6	6.933±0.195	0.401±0.012
2.8	6.473±0.140	0.387±0.004
3.0	5.529±0.099	0.383±0.010
3.2	7.699±0.092	0.401±0.015
3.4	7.908±0.132	0.410±0.008
3.6	8.134±0.093	0.433±0.006

*5 replications, RSD < 4 %

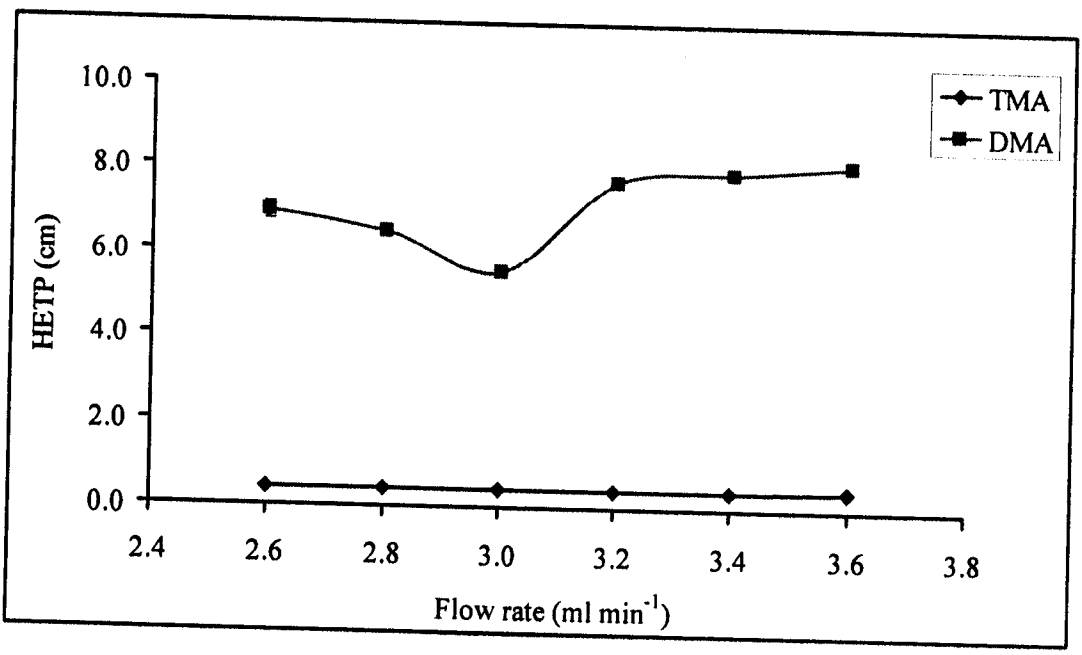

Figure 3.3 The van Deemter plot of DMA and TMA

3.1.2 Column temperature programming

Column temperature is one of the most important parameter in gas chromatography. The column temperature was first operated under isothermal temperature, 120°C but it took a long time to separate DMA and TMA. Therefore, a column temperature program was investigated.

The optimization of column temperature programming started with initial temperature and the results are shown in Table 3.2 and Figure 3.4. The analysis time also decreased when the temperature increased. The initial temperature at 120°C provides the highest response and a good separation and this was chosen.

Table 3.2 Effect of initial temperature on the responses of DMA (100 μg mL^{-1}) and was TMA (1 μg mL^{-1}) standard solution

Temperature (°C)	Responses×10^4 (μV)*	
	DMA	TMA
90	4.04±0.04	14.35±0.12
100	5.13±0.11	15.26±0.18
110	6.36±0.05	16.98±0.24
120	9.98±0.29	18.30±0.43
130	7.96±0.19	14.19±0.07

*5 replications, RSD < 4 %

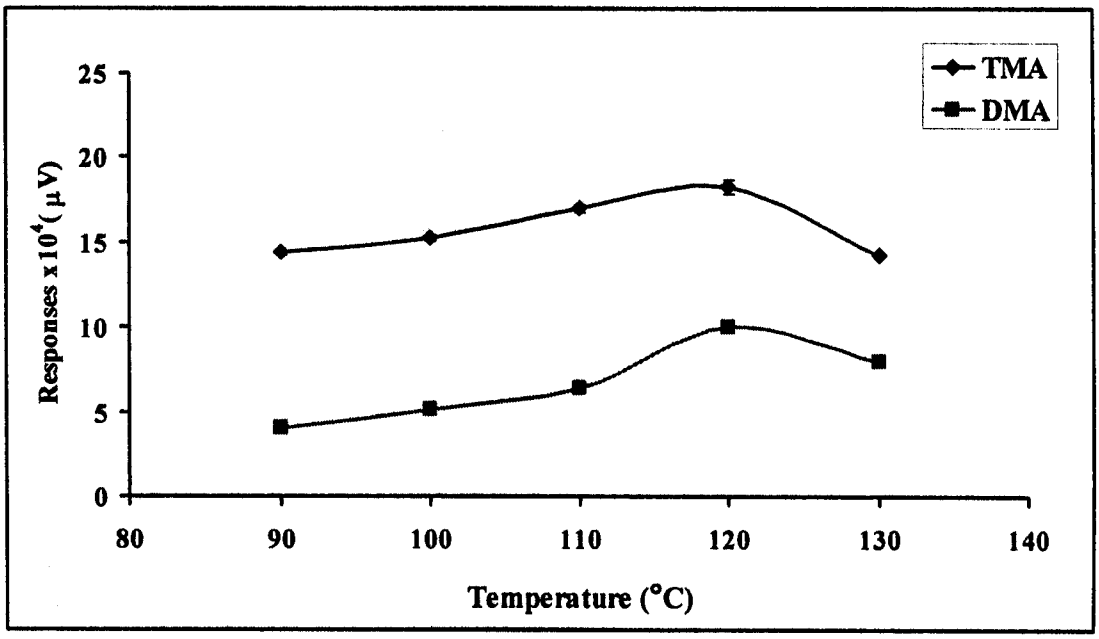

Figure 3.4 Responses of DMA (100 μg mL^{-1}) and TMA (1 μg mL^{-1}) standard solution at various initial temperatures

Holding time at initial temperature of 120°C was investigated and the results are shown in Table 3.3 and Figure 3.5. The responses decrease as the holding time increased for DMA because the responses of DMA had a tailing peak but the responses for TMA between 0 and 3 minutes were similar. Then 0 minute was chosen as the optimum.

Table 3.3 Effect of holding time at initial temperature on the responses of DMA (100 μg mL^{-1}) and TMA (1 μg mL^{-1}) standard solution

Time (min)	Responses×10^4 (μV)*	
	DMA	TMA
0	9.24±0.12	14.54±0.02
1	3.79±0.07	14.06±0.13
2	2.13±0.07	13.99±0.36
3	1.99±0.05	14.30±0.17

*5 replications, RSD < 4 %

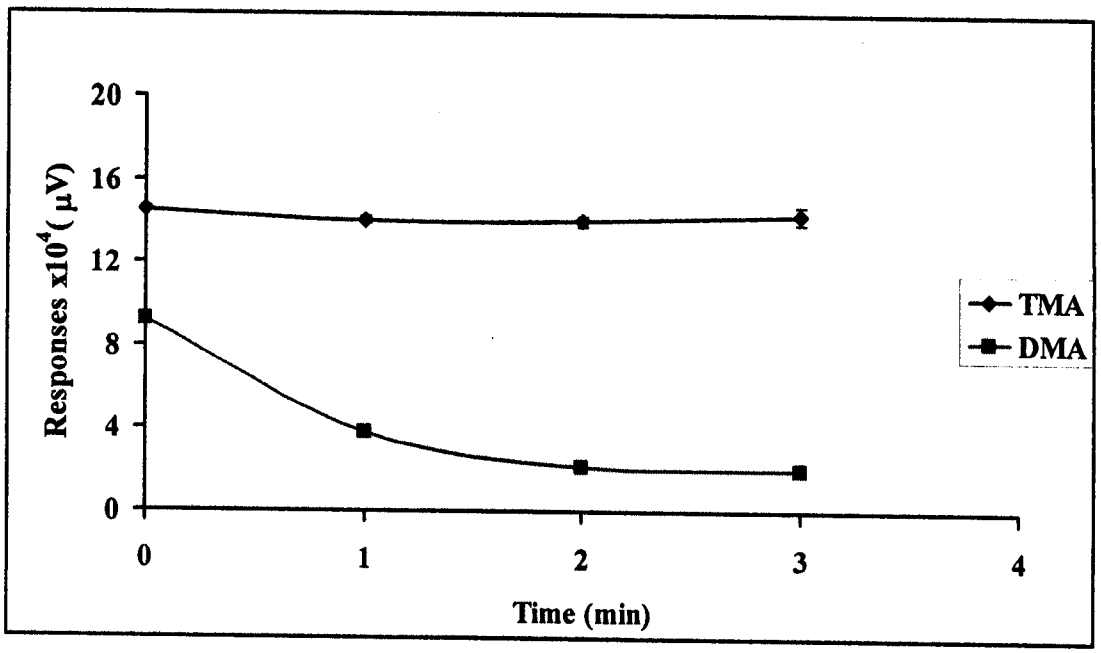

Figure 3.5 Responses of DMA (100 μg mL^{-1}) and TMA (1 μg mL^{-1}) standard solution at various holding time

The temperature ramp rate of temperature was investigated between 10-40°C min^{-1} as shown in Table 3.4 and Figure 3.6. After 30°C min^{-1} the responses differed less than 10% for DMA and TMA. For this reason, the temperature ramp rate

of 30°C min^{-1} was selected as the optimum since it provided good separation and short analysis time.

Table 3.4 Effect of temperature ramp rate on the responses of DMA (100 μg mL^{-1}) and TMA (1 μg mL^{-1}) standard solution

Temperature ramp rate (°C min^{-1})	Responses×10^4 (μV)*	
	DMA	TMA
10	2.92±0.10	14.21±0.23
20	3.53±0.11	12.86±0.08
25	4.81±0.09	13.07±0.16
30	7.98±0.13	14.91±0.39
35	7.71±0.12	14.29±0.39
40	7.63±0.05	13.73±0.29

*5 replications, RSD < 4 %

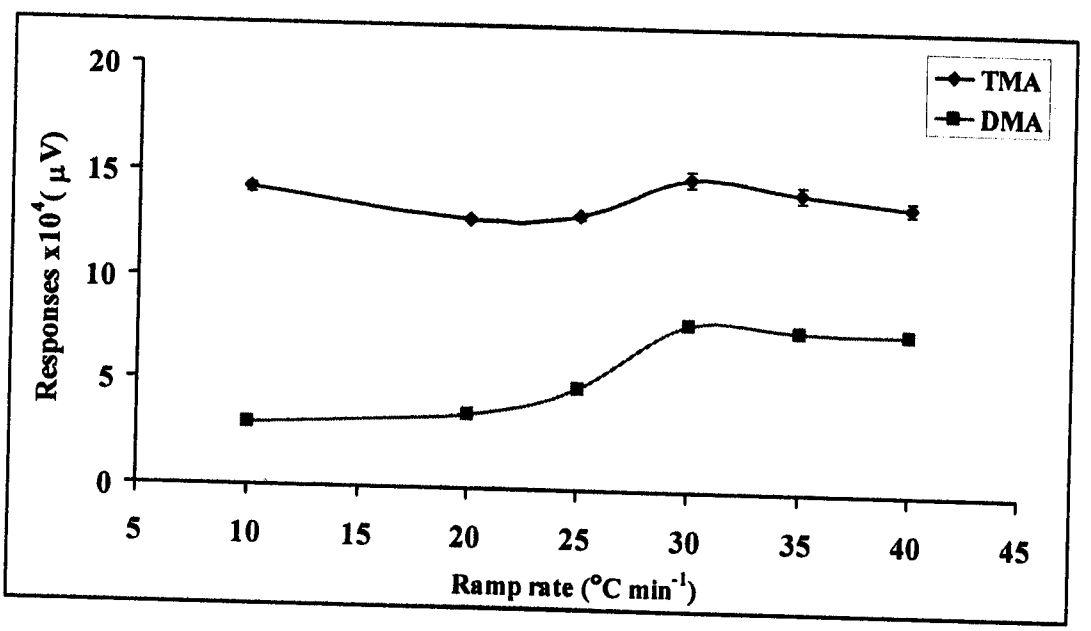

Figure 3.6 Responses of DMA (100 μg mL^{-1}) and TMA (1 μg mL^{-1}) standard solution at various temperature ramp rates

The optimum final temperature was investigated between 140°C and 180°C (Table 3.5 and Figure 3.7). The highest response was found at 160°C and this was select for the optimum final temperature.

Table 3.5 Effect of final temperature on the responses of DMA (100 μg mL^{-1}) and TMA (1 μg mL^{-1}) standard solution

Final temperature (°C)	Responses×10^4 (μV)*	
	DMA	TMA
140	5.95± 0.18	12.49 ± 0.41
150	4.71± 0.05	12.23±0.45
160	7.24± 0.04	13.25±0.18
170	3.69± 0.06	12.51±0.32
180	2.96± 0.11	12.29±0.33

*5 replications, RSD < 4 %

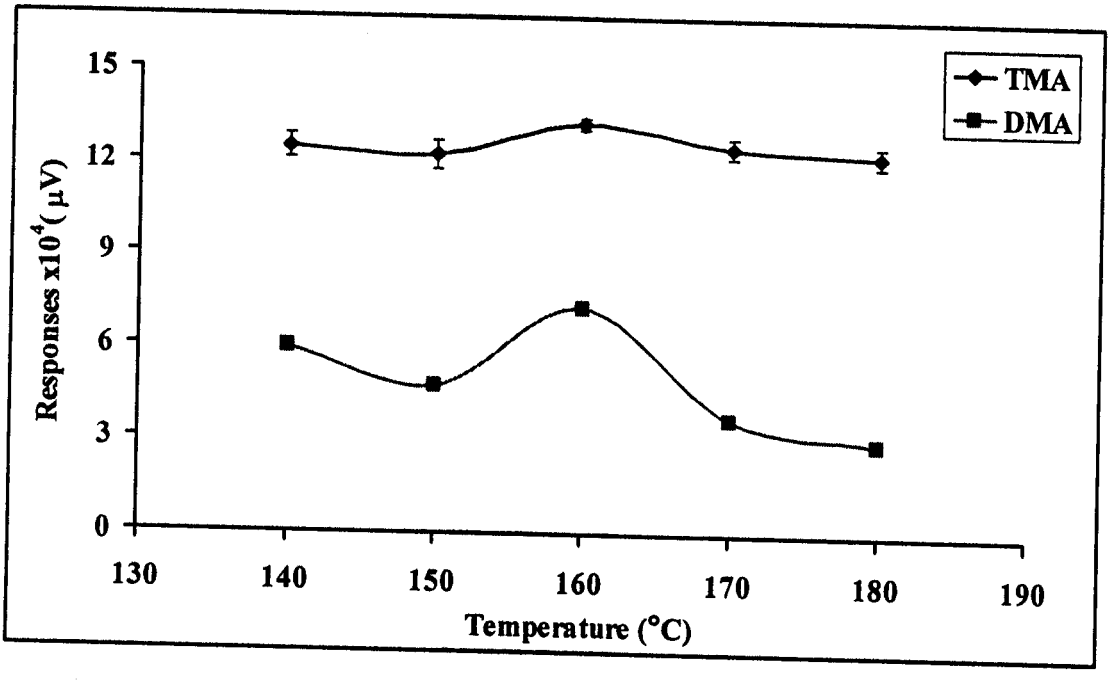

Figure 3.7 Responses of DMA (100 μg mL^{-1}) and TMA (1 μg mL^{-1}) standard solution at various final temperatures

After final temperature was investigated its holding time was obtained by considering the time that DMA and TMA could be completely eluted from the column. The holding time of final temperature at zero minute was not tested because it gave a DMA response with a tailing peak and did not allow the signal to go back to baseline. The optimum holding time at final temperature was investigated from 1-4 minutes. The results showed that the responses at holding time between 1 and 4 minutes differed less than 10% (Table 3.6 and Figure 3.8). Therefore, the holding time at final temperature of 1 minute was chosen to decrease analysis time at final temperature.

Table 3.6 Effect of holding time at final temperature on the responses of DMA (100 $\mu g\ mL^{-1}$) and TMA (1 $\mu g\ mL^{-1}$) standard solution

Holding time at final temperature (°C)	**Responses×10^4 (μV)***	
	DMA	**TMA**
1	6.02± 0.06	13.93 ± 0.21
2	6.43± 0.15	14.28± 0.35
3	5.78± 0.14	13.80± 0.13
4	5.21± 0.10	13.31± 0.30

*5 replications, RSD < 4 %

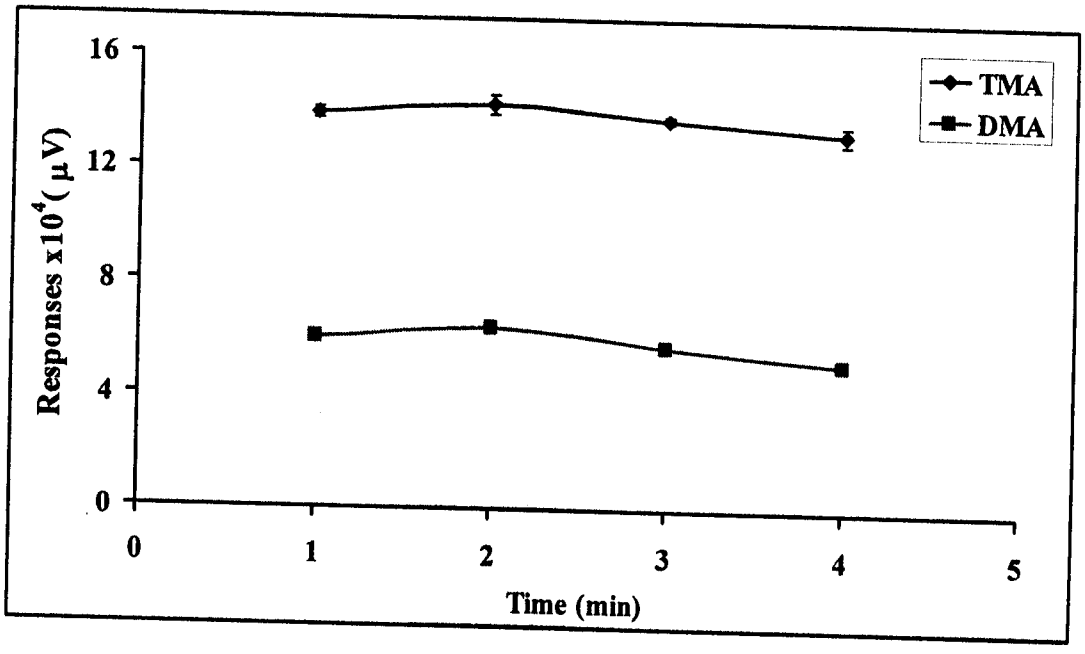

Figure 3.8 Responses of DMA (100 μg mL^{-1}) and TMA (1 μg mL^{-1}) standard solution at various holding time at final temperatures

The optimum conditions of column temperature programming for GC-NPD were summarized in Figure 3.9.

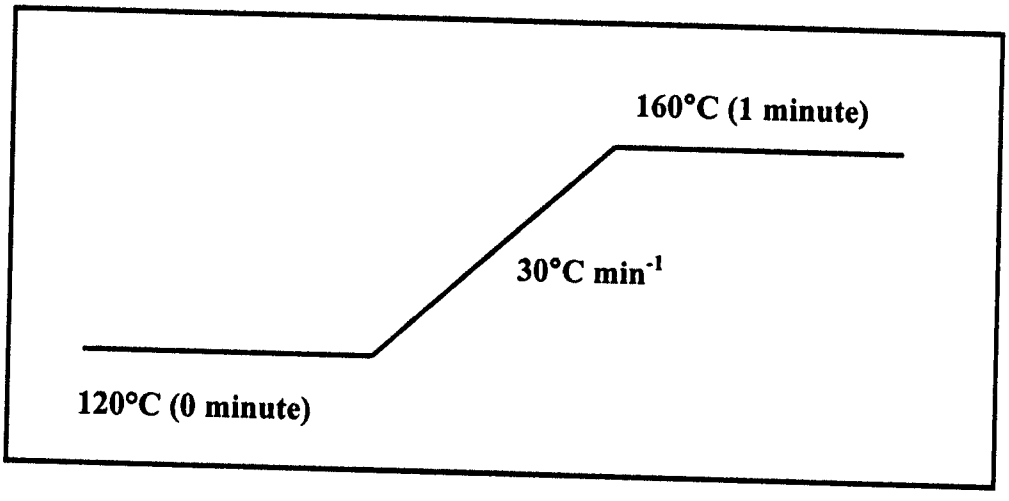

Figure 3.9 The optimum column temperature programming for DMA and TMA analysis

3.1.3 Injector temperature

Injector is an important part of the system that performs the physical task of transferring the sample into the gas chromatograph. The injector temperature must be high enough to vaporize the injected sample into the column but not too high that cause the sample components to decompose. The inlet injection of this study used a split mode where the split inlet allows the introduction of a user-selectable fraction of the injected sample into the capillary column by adjusting the relative flows of carrier gas into the column and to waste through a purge valve. Split inlet is heated, with a high thermal mass, to ensure that the entire injected sample evaporates quickly and mixes homogeneously with the carrier gas (Grob, 2004).

Table 3.7 and Figure 3.10 show the responses of DMA and TMA at injector temperature from 140-180°C where the responses differed less than 10%. By considering high resolution, short analysis time, and decrease tailing peak for DMA, 160°C was chosen as the optimum injector temperature.

Table 3.7 Effect of injector temperature on the responses of DMA (100 μg mL^{-1}) and TMA (1 μg mL^{-1}) standard solution

Injector temperature (°C)	**Responses×10^4 (μV)***	
	DMA	**TMA**
140	4.00±0.06	11.54 ± 0.38
150	4.28±0.12	11.57± 0.33
160	4.46±0.09	12.10± 0.45
170	4.25±0.15	11.96± 0.23
180	4.27±0.07	11.95± 0.39

*5 replications, RSD < 4 %

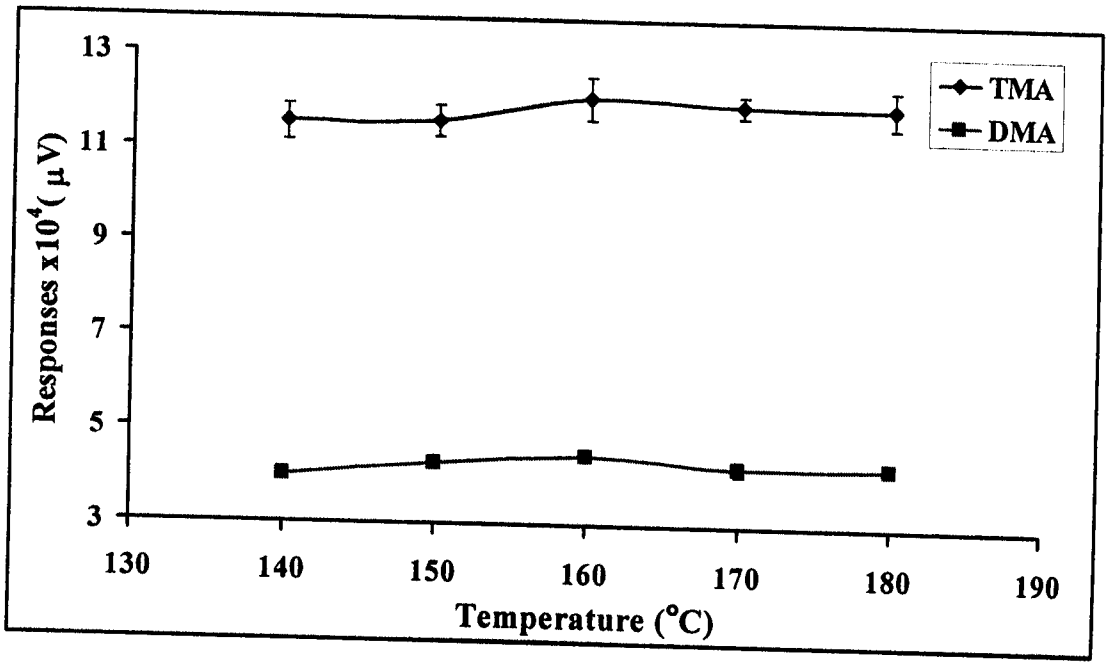

Figure 3.10 Responses of DMA (100 μg mL^{-1}) and TMA (1 μg mL^{-1}) standard solution at various injector temperatures

3.1.4 Detector temperature

The detection system in gas chromatography provides the responses signal for the chemical compounds separated by the chromatographic column. The type of detector used depended on the application. In this system the analytes eluted from the column was detected by the nitrogen phosphorous detector (NPD). The NPD is based on the phenomenon that a metal anode emits positive ions when heated in a gas. It is a commonly used gas chromatographic detector for the selective determination of organic compounds containing nitrogen (N) and phosphorous (P) atom.

The detectability and the specificity of the detector are both affected by the magnitude of the heating current. The hydrogen flow affects the concentration of the hydrogen atoms in the reactive gaseous layer around the thermionic source that in turn determines the responses. The effect of the flow rate and the temperature increased the source heating current beyond the base value required to initiate the H_2/air chemistry can increase the detectability of the detector (Grob, 2004).

The hydrogen and make up gases mix with the column effluent inside the jet. The gases leave the jet and mix with air; then, they are heated at the hot thermionic source, where decomposition and ionization occur. Ions are then collected at the collector electrode, which is maintained at a potential of a few hundred volts (Grob, 2004).

The responses from various detector temperatures are shown in Table 3.8 and Figure 3.11. Although 240°C gave the highest response but the limit of the column temperature was at 250°C therefore 220°C was chosen as the optimum detector to avoid damaging the column.

Table 3.8 Effect of detector temperature on the responses of DMA (100 μg mL^{-1}) and TMA (1 μg mL^{-1}) standard solution

Detector temperature (°C)	**Responses×10^4 (μV)***	
	DMA	**TMA**
180	2.27±0.07	7.23 ± 0.22
200	2.40±0.06	8.76± 0.11
210	2.86±0.07	9.04± 0.20
220	2.93±0.10	9.56± 0.35
230	2.86±0.12	10.11±0.49
240	3.82±0.09	11.27± 0.20

*5 replications, RSD < 4 %

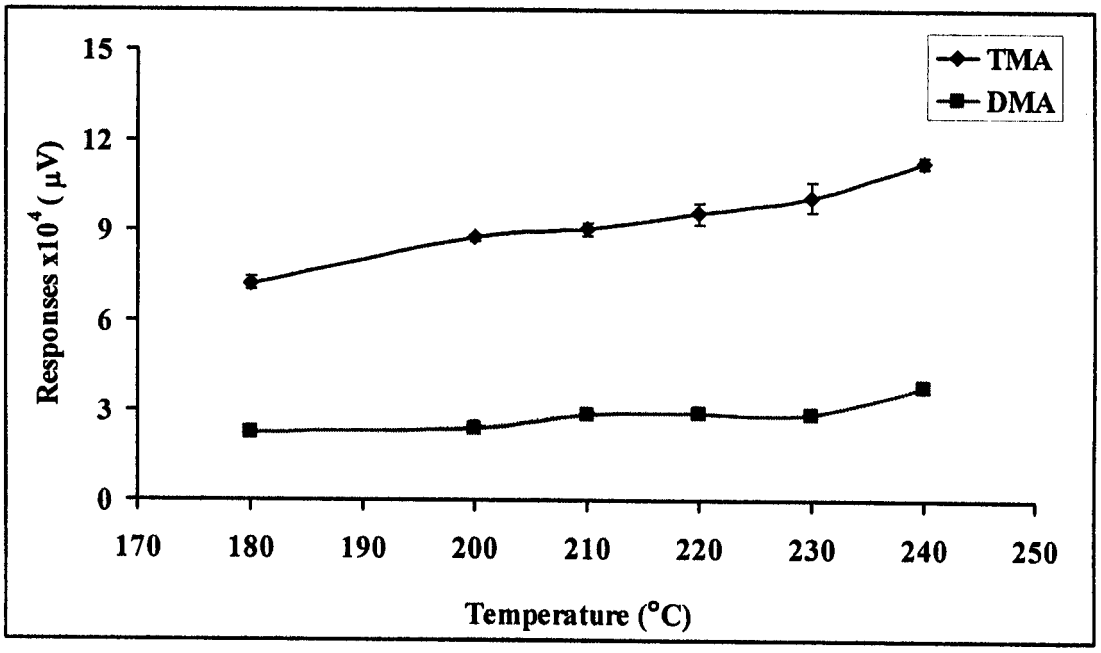

Figure 3.11 Responses of DMA (100 μg mL^{-1}) and TMA (1 μg mL^{-1}) standard solution at various detector temperatures

3.1.5 The fuel gas flow rate (hydrogen gas)

The design of the nitrogen phosphorous detector used in this work is similar to a flame ionization detector (FID) but with an important difference *i.e.*, an electrically heated silicate bead doped with an alkali salt was mounted between the jet and the collector. A very low hydrogen gas flow rate is mixed with the carrier gas and burns as plasma flame when contact with the heated bead and jet. The exact mechanism for producing a responses has been subject of some discussion, but Kolb's theory seems to be widely accepted (Tripler, 1993). At the operating temperature, the bead substrate is electrically conductive and some of the alkali ions are able to acquire an electron and are thus converted to the atomic form. These atoms are relatively volatile and are emitted into the plasma, where they quickly react with combustion products, and are ionized again and recollected on the negatively polarized bead. This repeated process gives rise to the background signal and explains why the bead continues to function over an extended time. When a compound containing nitrogen or phosphorous eluted from the column into the plasma, these molecules will burn and

react with the exited atomic alkali to form phosphorous oxide anions. These reactions disturb the alkali equilibrium in the plasma and additional alkali released into the plasma, thus promoting further ion formation and in creasing the signal (Baugh, 1993).

The main disadvantage of this detector is that its performance deteriorates with time. The alkali salt employed as the bead is usually an alkali silicate that the reduced responses was due to water vapour from the burning hydrogen, converting the alkali silicate to the hydroxide. At the operating temperature of the bead, the alkali hydroxide has significant vapour pressure and consequently, the rubidium or cesium is continually lost during the operating of the detector. Eventually all the alkali is evaporated, leaving a bead of inactive silica. This an inherent problem with all NPD detectors and as a result, the bead needs to place regularly if the detector is in continuous use (Raymond, 1998).

In this system the analyte eluted from the column was detected by a nitrogen phosphorous detector (NPD). The detector consists of small hydrogen and air diffusion flame burning produced from oxidant and fuel gas. The oxidant gas was air and fuel gas was hydrogen. Thus, the flow rate of air and hydrogen gases significant influences the noise level and the sensitivity of the detector.

The effect of hydrogen gas flow rate to the responses is shown in Table 3.9 and Figure 3.12. The highest response was obtained at 2.0 mL min^{-1}, the optimum flow rate. This is the same as the recommended value of GC-NPD manual, 2.0 mL min^{-1} (The Perkin-Elmer Corporation, 1995).

Table 3.9 Effect of hydrogen gas flow rate on the responses of DMA (100 μg mL^{-1}) and TMA (1 μg mL^{-1}) standard solution

Hydrogen gas flow rate (mL min^{-1})	Responses×10^4 (μV)*	
	DMA	TMA
1.0	3.57 ± 0.13	9.71 ± 0.20
2.0	7.06 ± 0.12	11.51 ± 0.20
3.0	4.90 ± 0.12	7.99 ± 0.17
4.0	4.48 ± 0.05	6.21 ± 0.06

*5 replications, RSD < 4 %

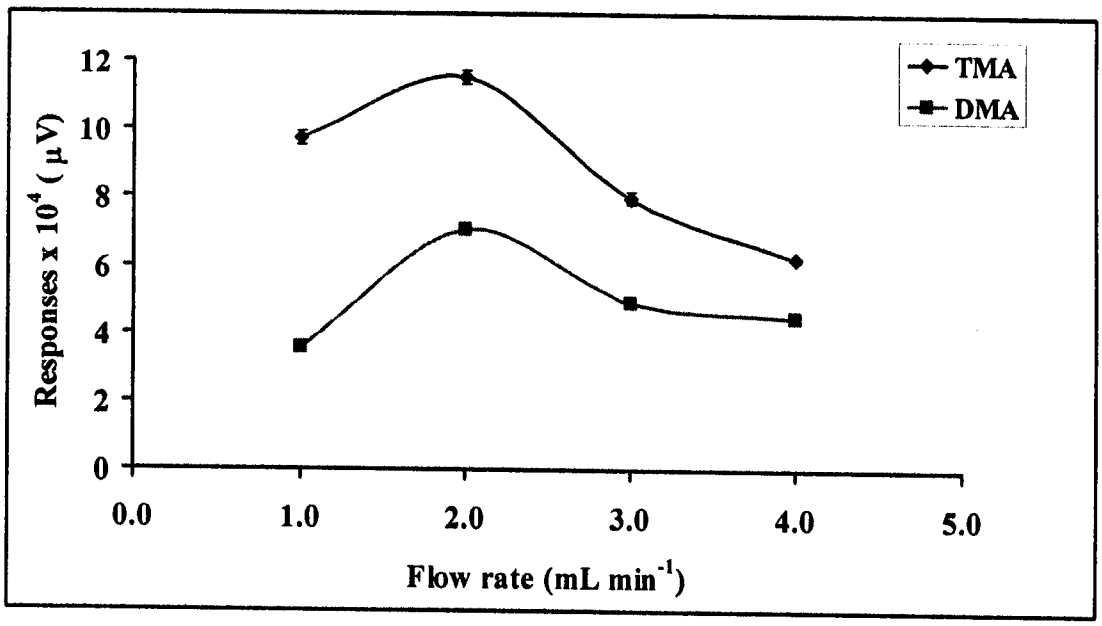

Figure 3.12 Responses of DMA (100 μg mL^{-1}) and TMA (1 μg mL^{-1}) standard solution at various hydrogen gas flow rates

3.1.6 Oxidant gas flow rate (air)

Air was used as an oxidant for NPD. Typical flows of air are 100-200 mL min^{-1} (Grob, 2004). The effect of air flow rate on the responses (section 2.6.3) is

shown in Table 3.10 and Figure 3.13. The highest response was obtained at 100 mL min^{-1}, the same as the recommend value of GC-NPD manual (The Perkin-Elmer Corporation, 1995).

Table 3.10 Effect of air flow rate on the responses of DMA (100 μg mL^{-1}) and TMA (1 μg mL^{-1}) standard solution

Air flow rate (mL min^{-1})	Responses×10^4 (μV)*	
	DMA	TMA
90	2.88 ± 0.09	10.37 ± 0.34
100	4.82 ± 0.18	16.62 ± 0.39
110	4.55 ± 0.11	14.43 ± 0.28
120	4.29 ± 0.15	12.46 ± 0.32

*5 replications, RSD < 4 %

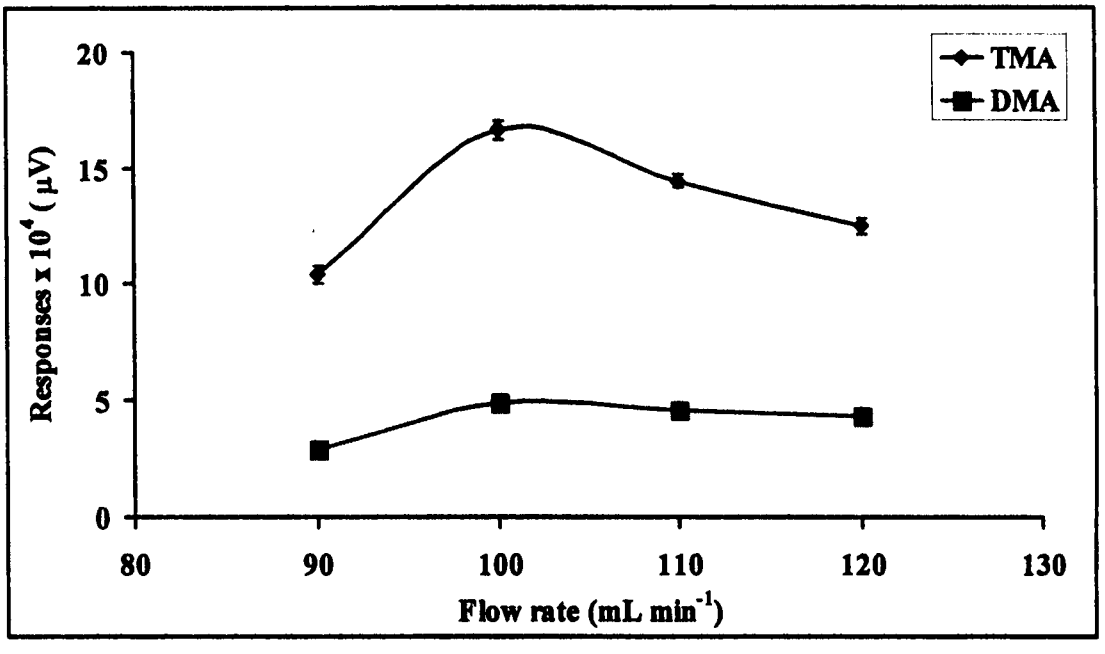

Figure 3.13 Responses of DMA (100 μg mL^{-1}) and TMA (1 μg mL^{-1}) standard solution at various air flow rates

3.1.7 The split ratio

The split ratio is the ratio of the volumetric flow rate at the split purge vent to the volumetric flow rate in the GC column.

Preliminary study showed that at the split ratio less than 10:1 although a high response was obtained, it provided broad peaks and the resolution was less than one because the analytes overload the capillary column. When increase the split ratio from 10:1 up to 40:1 the responses of DMA and TMA decreased (Table 3.11, Figure 3.14) because less analytes flowed through the capillary column. The optimum split ratio was then selected at 10:1 because it gave the highest response and the resolution was higher than others.

Table 3.11 Effect of the split ratio on the responses of DMA (100 μg mL^{-1}) and TMA (1 μg mL^{-1}) standard solution

The split ratio	**Responses×10^4 (μV)***	
	DMA	**TMA**
10	8.87±0.14	12.09±0.06
20	3.81±0.13	7.26±0.16
30	2.16±0.03	4.71±0.14
40	2.07±0.03	4.34±0.11

*5 replications, RSD < 4 %

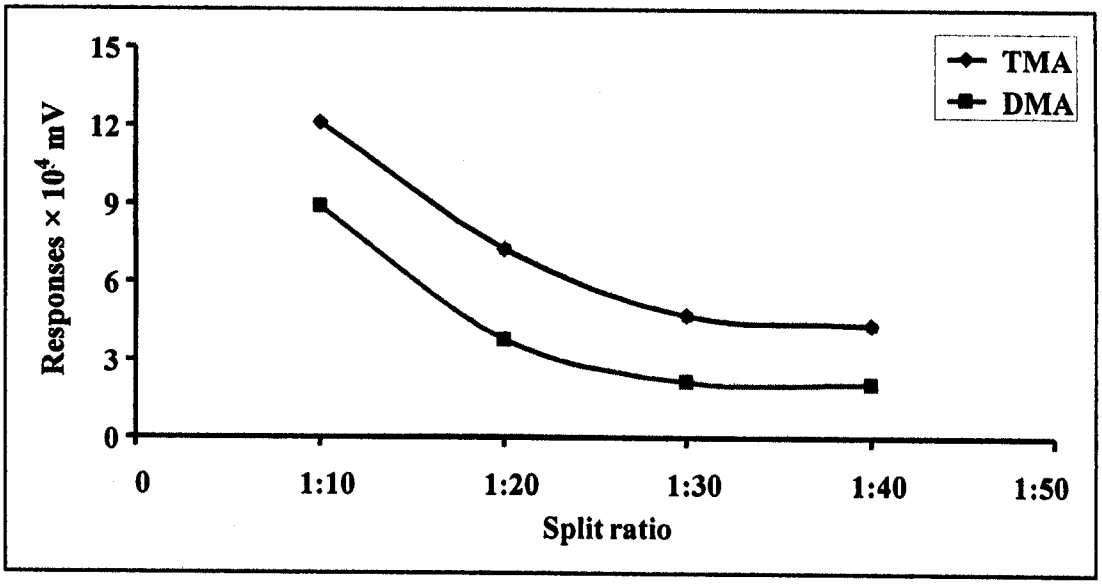

Figure 3.14 Responses of DMA (100 μg mL^{-1}) and TMA (1 μg mL^{-1}) standard solution at various the split ratios

3.1.8 Summary of GC-NPD conditions

The optimum conditions for DMA and TMA analysis on capillary column (HP-FFAP, 25 m × 0.32 mm i.d., 0. 52 μm film thicknesses) with nitrogen phosphorous detector are summarized in Table 3.12. The chromatogram obtained from these optimum conditions is shown in Figure 3.15.

Table 3.12 The optimum conditions of GC-NPD for DMA and TMA

Conditions	Optimum conditions
Flow rate	
- Carrier gas (helium gas)	3 mL min^{-1}
- Fuel flow rate (hydrogen gas)	2 mL min^{-1}
- Oxidant gas flow rate (air)	100 mL min^{-1}
Column temperature programming	
- Initial temperature	120°C
- Holding time at initial temperature	0
- Temperature ramp rate	30°C min^{-1}
- Final temperature	160°C
- Holding time at final temperature	1 min
Injector temperature	160°C
Detector temperature	220°C
Split ratio	1:10

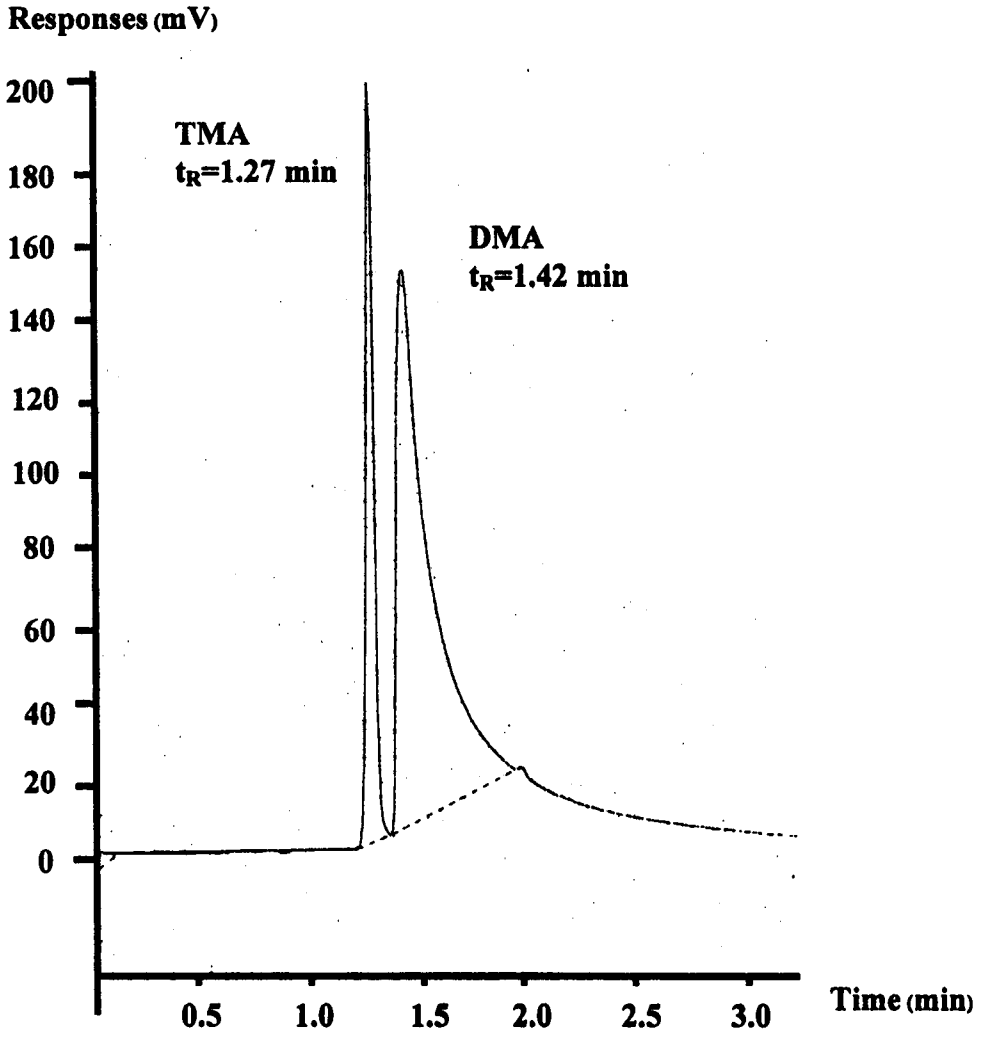

Figure 3.15 The chromatogram of DMA (100 μg mL^{-1}) and TMA (1 μg mL^{-1}) at optimum GC-NPD conditions

3.1.9 Headspace analysis conditions

Headspace gas chromatography (GC-NPD) has been available since the late 1960s (Hachenberg *et al.*, 1977) and is a rugged, robust and popular method of sample preparation used for the introduction of volatile analytes to gas chromatograph. There are two types of headspace analysis: static and dynamic. In static analysis, the analytes are samples under conditions of equilibration and in dynamic; the analytes are exhaustively extracted from the sample (purge and trap).

For static headspace, the sample is sealed in a vial where the analytes reach equilibrium between the gas phase (headspace) and sample (liquid and solid). Once reach to equilibrium the analytes are transferred to the chromatograph for analysis. In dynamic headspace, equilibrium is never reached from the vial. The volatile analytes are swept to a trap where they held until analyses (Grob, 2004).

Static headspace was employed and the volatile DMA and TMA in the solution are present in the gas phase that is in contact with the solution of the headspace vial as shown in Figure 3.16. It relative concentrations in the gas phase depend on the partition pressure which in turn could be influenced by temperature and time (Kolb and Ettre, 1997).

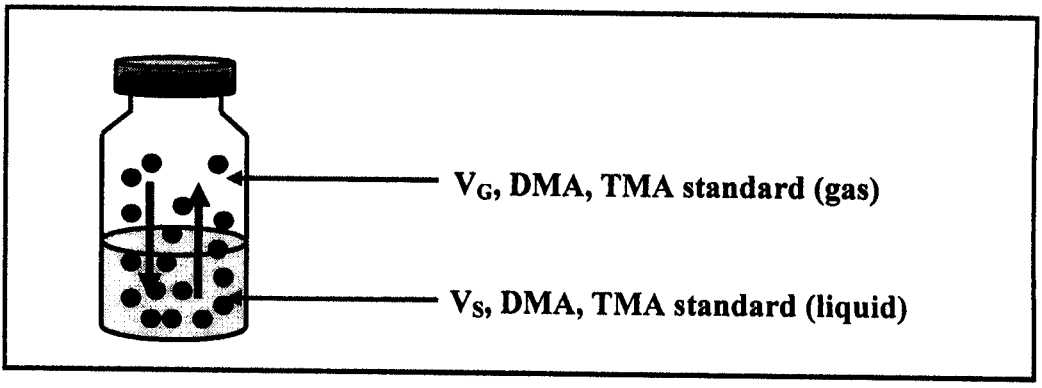

Figure 3.16 A headspace vial containing the volatile DMA and TMA in standard solution: V_G = volume of the gas phase, V_S = volume of the liquid sample

3.1.10 Equilibration temperature

The influence of equilibration temperature on the volatility and the headspace sensitivity were studied. In static headspace analysis increasing temperature to enhance sensitivity could cause a condensation problem from the evaporation of the analyte into gas phase. Therefore, the equilibration temperature should be optimized to avoid the condensation. For the laboratory-built thermal system at temperature higher than 70°C, condensation of analyte in the syringe occurred during the transfer of the gas phase headspace to GC-NPD system. To avoid

this condensation, ASTM standard practice recommended the syringe should be heated it in the oven at 90°C before sampling (Kolb and Ettre, 1997). In this work the syringe was cleaned by a syringe cleaner and heated at 370°C.

The effects of the equilibration temperature on the responses are shown in Table 3.13 and Figure 3.17. The responses of DMA and TMA increased when the equilibration temperature increased. The equilibration temperature at 70°C that gave the highest response and sensitivity without condensation.

Table 3.13 Effect of equilibration temperature on the responses of DMA (100 μg mL^{-1}) and TMA (1 μg mL^{-1}) standard solution

Equilibration temperature (°C)	**Responses×10^4 (μV)***	
	DMA	**TMA**
40	10.91±0.10	4.27±0.03
50	16.23±0.15	10.51±0.29
60	16.69±0.46	18.67±0.10
70	16.78±0.15	26.83±0.81
80	17.20±0.01	44.45±1.56

*5 replications, RSD < 4 %

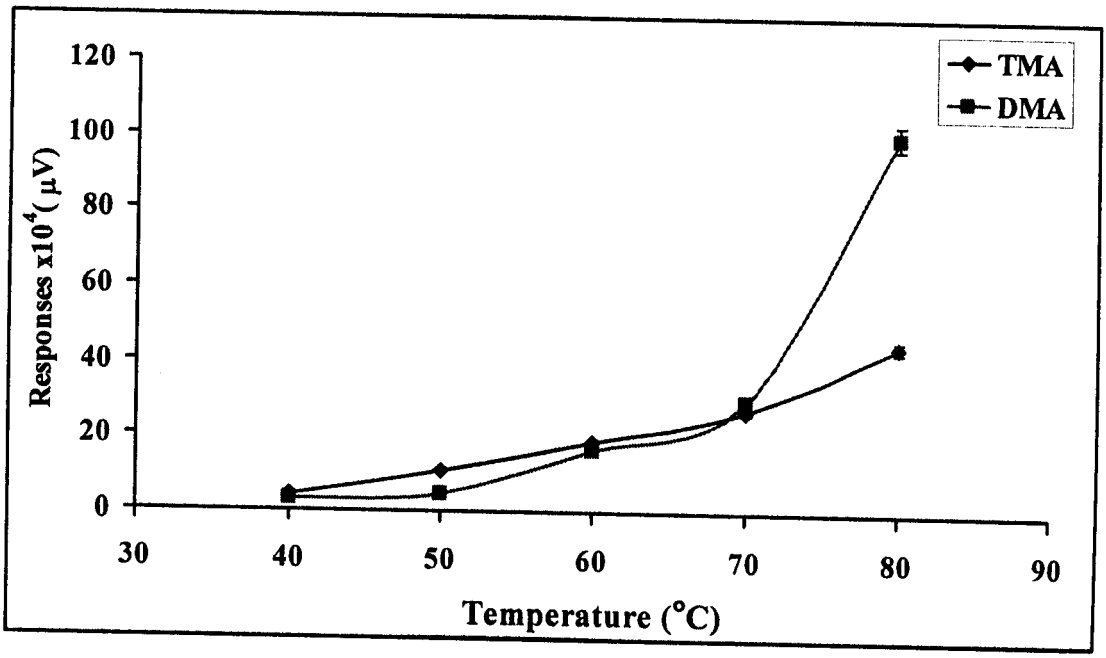

Figure 3.17 Responses of DMA (100 μg mL^{-1}) and TMA (1 μg mL^{-1}) standard solution at various equilibration temperatures

3.1.11 Equilibration time

Parameters influencing the headspace sensitivity are equilibration temperature, equilibration time and sample volume (phase ratio). The equilibration time is depending on the distribution of volatile components. For this work, headspace technique for the standard DMA and TMA solutions is performed by placing the sample in a closed headspace vial to establish an equilibrium condition between the sample and gas phases in a laboratory-built thermal bath system. DMA and TMA were continuously extracted from the liquid phase (sample phase) into gas phase until an equilibration was reached (DMA and TMA in the gas phase equal to the DMA and TMA in the liquid phase). Table 3.14 and Figure 3.18 showed that the responses increased with equilibration time up to 20 minutes and became constant. Therefore, 20 minutes was selected as the optimum equilibration time.

Table 3.14 Effect of equilibration time on the responses of DMA (100 μg mL^{-1}) and TMA (1 μg mL^{-1}) standard solutions

Equilibration time (min)	Responses×10^4 (μV)*	
	DMA	TMA
10	10.91±0.10	20.80±0.43
20	16.23±0.15	22.33±0.21
30	16.69±0.46	22.57±0.49
40	16.78±0.15	23.00±0.34
50	17.20±0.01	23.12±0.63

*5 replications, RSD < 4 %

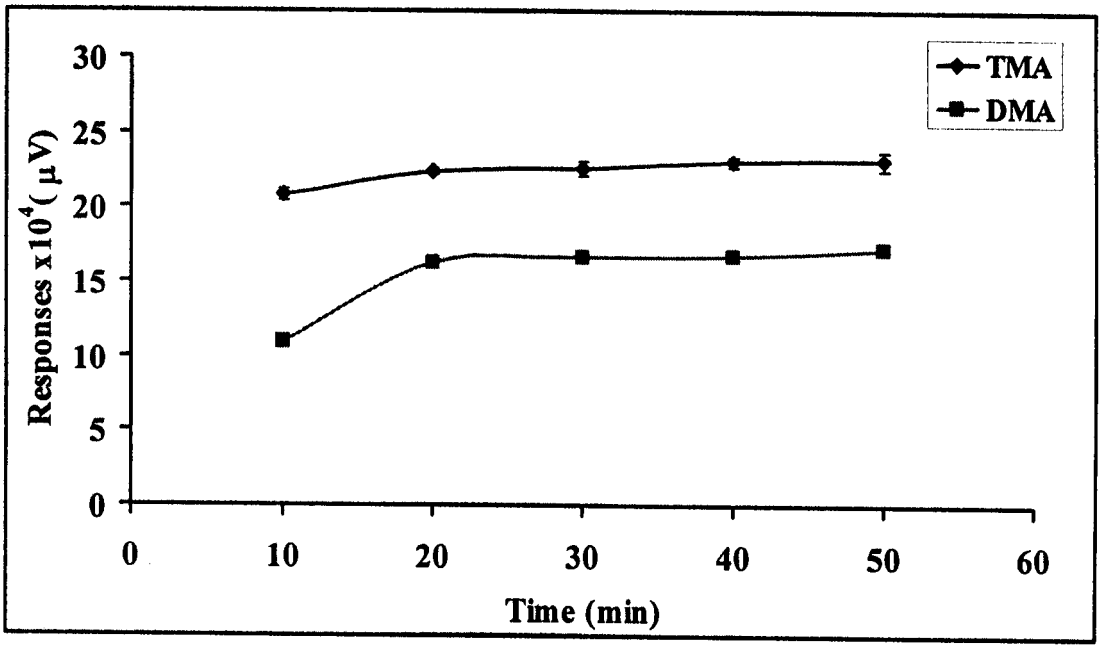

Figure 3.18 Responses of DMA (100 μg mL^{-1}) and TMA (1 μg mL^{-1}) standard solution at various equilibration times

3.1.12 Sample volume (phase ratio)

The headspace sensitivity also depends on the phase ratio. The phase ratio (β) is the ratio of the volume of the gas phase to the volume of the sample phase in the vial (Figure 3.16) and is presented as equation 3.7.

$$\beta = \frac{V_G}{V_S} \tag{3.7}$$

Where V_G = volume of the gas phase

V_S = volume of the sample phase

V_V = volume of the total

When

$$V_V = V_G + V_S \tag{3.8}$$

equation (3.7) can be expressed as

$$\beta = \frac{V_V - V_S}{V_S} \tag{3.9}$$

and

$$V_S = \frac{V_V}{1+\beta}. \tag{3.10}$$

Therefore

$$\beta = \frac{V_G}{V_S} = \frac{V_V - V_S}{V_S} = \frac{V_G}{V_V - V_G} \tag{3.11}$$

The phase ratio will increase when the sample volume decrease or gas phase increase.

Headspace analysis is also related to the distribution of analyte between the two phases upon the equilibrium and is expressed by the

thermodynamically controlled equilibrium constant. In analogy to the common practice in gas chromatography, the synonymous term partition (distribution) coefficient, K, and is express as

$$K = \frac{C_S}{C_G} \tag{3.12}$$

Where K is the partition coefficient related to the mass distribution in the phase system. It depends on the solubility of the analyte in the condensed phase: compounds with high solubility will have a high concentration in the condensed phase relative to the gas phase. C_S is the concentration of analyte in sample phase (condensed phase). C_G is the concentration of analyte in gas phase (headspace).

Headspace analysis technique was used in this work and the responses of DMA and TMA using GC-NPD were measured as the peak height. The relation of the concentration of sample and peak height is expressed as equation 3.13

$$A \propto C_G = \frac{C_O}{K + \beta} \tag{3.13}$$

Where A = peak area (in this work was used peak height)

C_G = the concentration of the analyte in the headspace (gas phase)

C_O = the original sample concentration of the analyte

K = the partition coefficient

β = phase ratio of the vial

From equation (3.13) the headspace sensitivity (the peak height) is depended on the distribution coefficient (K) and phase ratio (β). The sensitivity of the headspace will increase as the distribution coefficient and phase ratio decrease.

The phase ratio for the headspace laboratory-built thermal bath system was investigated in section 2.7.3. The results are shown in Table 3.15 and Figure 3.19. The phase ratio at 1.0, 1.5 and 2.0 gave high responses and were nearly the same. The optimum phase ratio of headspace technique was chosen at 2.0 (20 mL sample volume in a 60 mL vial) because it used less sample volume. The phase ratio lower than 1.0 (0.2 and 0.5) gave less sensitivity because it did not reach thire equilibrium.

Table 3.15 Effect of phase ratio on the responses of DMA (100 μg mL^{-1}) and TMA (1 μg mL^{-1}) standard solutions

Phase ratio	Responses×10^4 (μV)*	
	DMA	TMA
0.2	12.42±0.15	14.97±0.50
0.5	16.56±0.37	16.32±0.46
1.0	19.77±0.72	19.12±0.52
1.5	19.29±0.48	18.91±0.22
2.0	18.53±0.21	18.79±0.54
5.0	15.84±0.39	16.76±0.23

*5 replications, RSD < 4 %

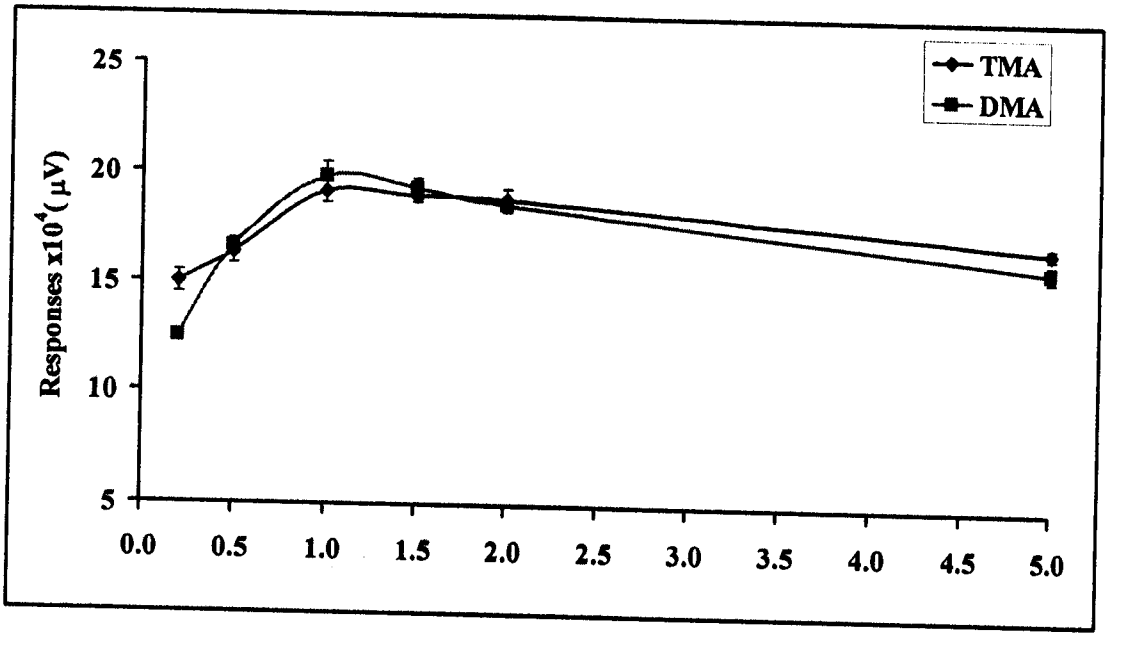

Figure 3.19 Responses of DMA (100 μg mL^{-1}) and TMA (1 μg mL^{-1}) standard solution at various phase ratios

3.1.13 Vial volume size

Three size of vial *i.e.*, 10, 30 and 60 mL were used for the investigation. The analyses of DMA and TMA in fish and shrimp samples with GC-NPD system are shown in Table 3.16 and Figure 3.20. The headspace sensitivity primarily depends on the concentration in the gas phase but not on the sample vial size: the phase ratio (β) is the one that determines the final sensitivity. The result showed that a 3.33 mL liquid sample in a 10 mL vial gave the highest response because a smaller sample volume allows shorter equilibrium vial (Kolb and Ettre, 1997) (The phase ratio, β in all cases was 2). Consequently, a 10 mL of vial volume was chosen to prepare sample.

Table 3.16 Effect of size of vial volume on the responses of DMA (100 μg mL^{-1}) and TMA (1 μg mL^{-1}) standard solution

Size of vial volume (mL)	Responses×10^4 (μV)*	
	DMA	TMA
10	2.37±0.13	0.93±0.04
30	1.14±0.12	0.59±0.02
60	0.75±0.06	0.69±0.08

*5 replications, RSD < 13 %

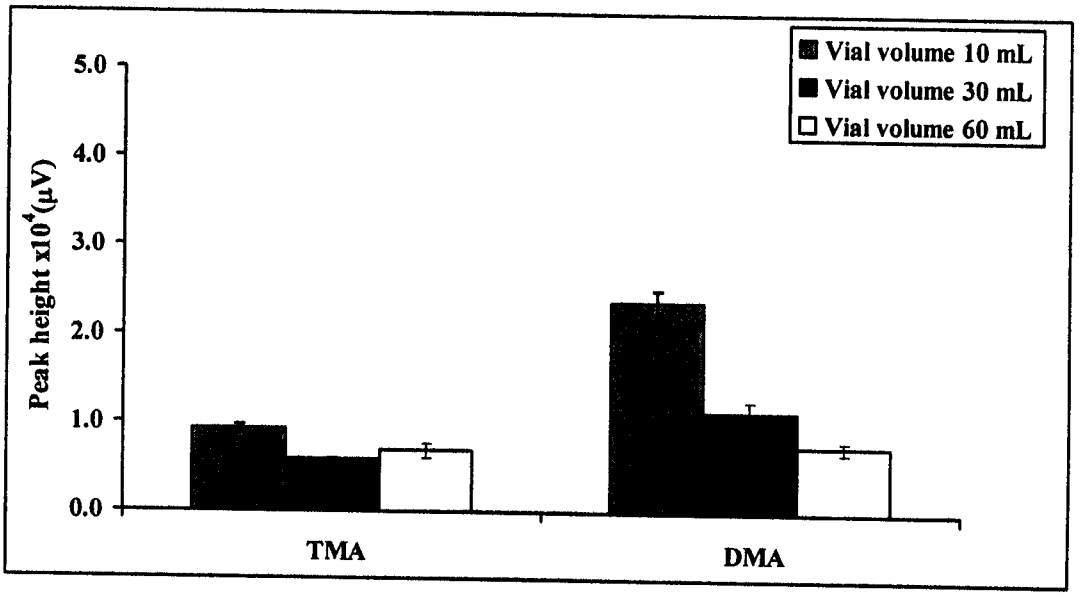

Figure 3.20 Responses of DMA (100 μg mL^{-1}) and TMA (1 μg mL^{-1}) standard solution at various size of vial volume

3.1.14 Salts and amount of salts

In headspace technique the activity coefficient can be increased by adding salt. A small partition coefficient indicates reduced the solubility of the analyte in the matrix and thus an increased concentration in the headspace in equation 3.12. This can be achieved by adding an electrolyte (salt) to the sample and the technique, commonly called salting out. However, the sensitivity is not influenced by salting out effect alone; there is an additional volume effect involved which is widely ignored (Kolb and Ettre, 1997). The addition of a high amount of salt increases the volume of liquid sample thus decreases the phase ratio (β).

In this work, the adding of NaCl, Na_2CO_3, Na_2SO_4 and KCl were tested where the amounts were varied at 0.5, 1.0, 1.5 and 2.0 g. The results are shown in Tables 3.17-3.18 and Figures 3.21-3.22. The salt and amount of salt that gave the highest response for both DMA and TMA was Na_2CO_3 at 1.5 g because it has the highest ionic strength which can be obtained from the Debye Hückel theory as equation 3.14 resuting in the decreasing of analytes solubility in the matrix. The other

reason is that sample under the addition of Na_2CO_3 is in the basic condition which kept the analyte in the original form.

$$I = \frac{1}{2}\sum_i C_i Z_i^2 \qquad (3.14)$$

Where I is ionic strength

C_i is the concentration of every ion, mol L^{-1}

Z_i are the charges on the two ions (Butler and Cogley, 1998).

The higher ionic strength can decrease the solubility of analyte in matrix resulting in higher concentration of the analyte in the gas phase (Kolb and Ettre, 1997).

So, the best salt and amount was Na_2CO_3 at 1.5 g that is the salting out to reduce the solubility of the analyte in the matrix.

Table 3.17 Effect of salt and amount of salt on the responses of DMA (150 μg mL^{-1}) standard solution

Amount of salt (g)	Responses×10^4 (μV)* for DMA			
	NaCl	Na_2CO_3	Na_2SO_4	KCl
0.5	48.4±1.3	345.4±4.7	42.7±1.6	37.3±1.0
1.0	39.4±1.3	501.8±10.8	70.2±2.4	48.8±1.2
1.5	96.9±2.2	1234.8±18.2	554.7±6.1	184.1±2.5
2.0	76.5±1.5	763.5±12.3	232.5±4.8	84.8±1.0

*5 replications, RSD < 4 %

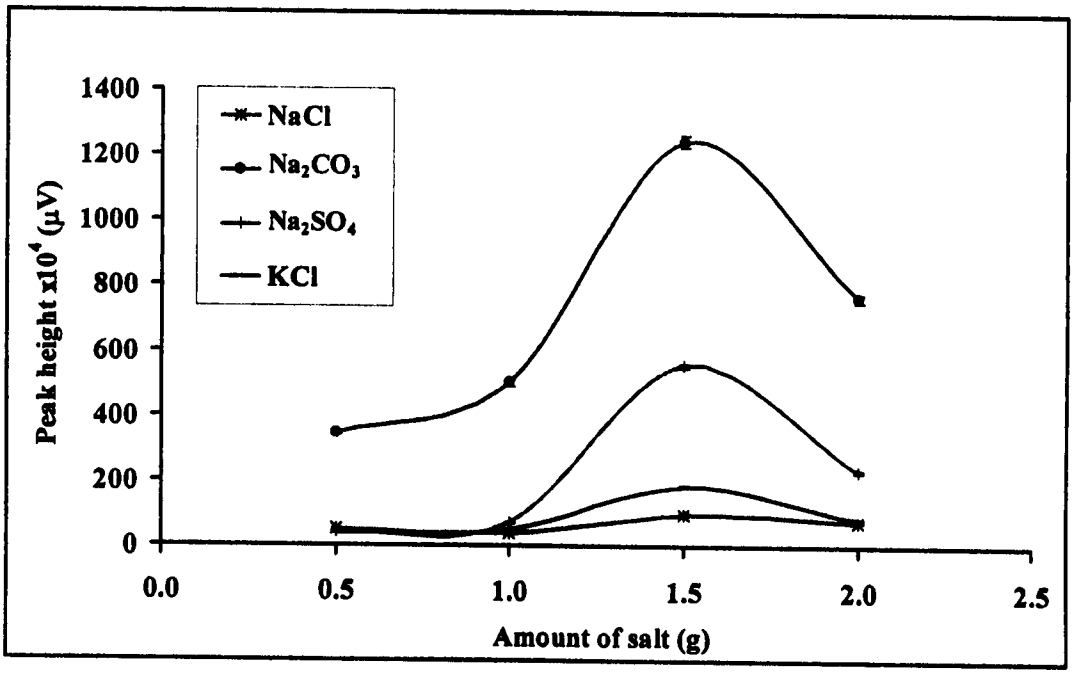

Figure 3.21 Responses of DMA (150 μg mL^{-1}) standard solution at various salts and amount of salt

Table 3.18 Effect of salt and amount of salt on the responses of TMA (1 μg mL^{-1}) standard solution

Amount of salt (g)	Responses×10^4 (μV)* for TMA			
	NaCl	Na_2CO_3	Na_2SO_4	KCl
0.5	17.7±0.5	36.7±1.4	19.5±0.8	15.7±0.2
1.0	35.3±1.3	51.2±2.0	41.5±1.4	33.4±0.8
1.5	29.8±0.9	112.8±0.6	70.8±1.7	40.4±0.6
2.0	19.8±0.6	67.7±1.1	43.4±1.4	30.2±0.7

*5 replications, RSD < 4 %

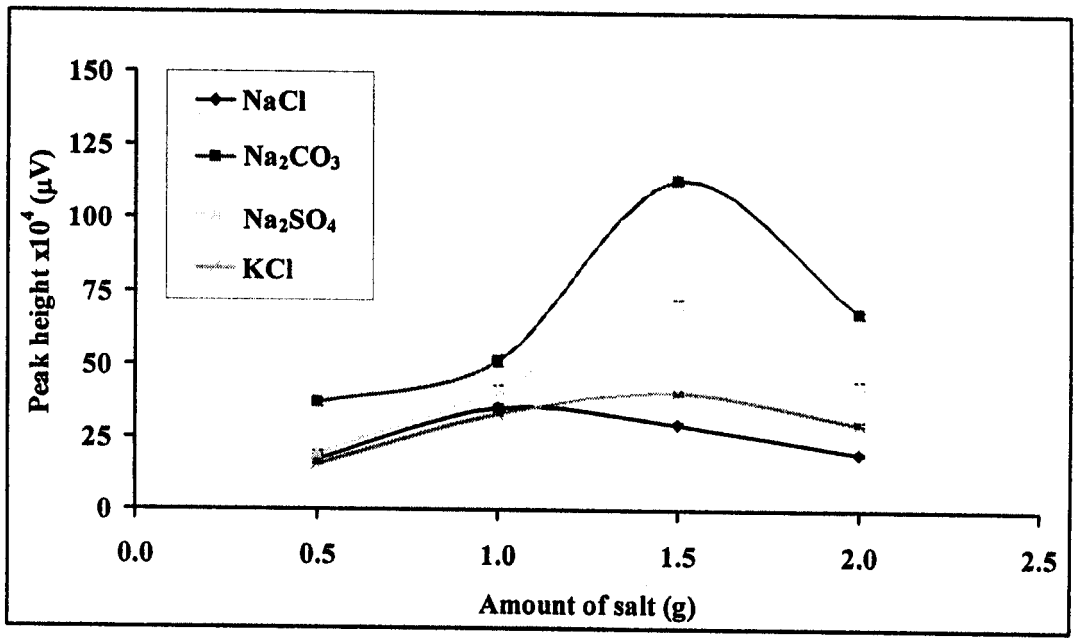

Figure 3.22 Responses of TMA (1 μg mL^{-1}) standard solution at various salts and amount of salt

3.1.15 Summary of headspace conditions

The optimum headspace conditions for the analysis of DMA and TMA in fish and shrimp samples with GC-NPD using HP-FFAP capillary column are summarized in Table 3.19. The chromatogram obtained by these conditions are shown in Figure 3.23 where the resolution more than one were obtained.

Table 3.19 The optimum conditions of headspace system for DMA and TMA analysis

Parameter	Optimum values
Headspace system	
• Equilibration time	20 minute
• Equilibration temperature	70°C
• Phase ratio	2.0
• Vial volume	10 mL
• Salt and amount of salt	Na_2CO_3 1.5 g

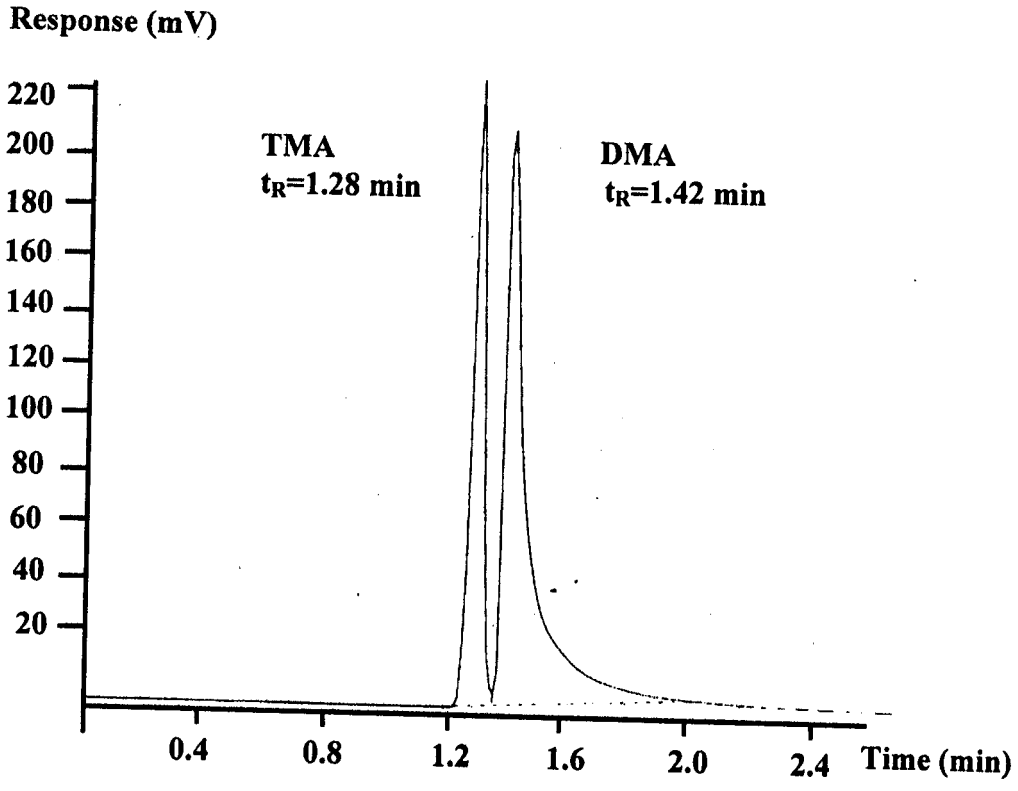

Figure 3.23 Chromatogram of TMA (1 μg mL^{-1}) and DMA (100 μg mL^{-1}) standard solution by HS-GC-NPD system

3.2 Linear dynamic range (LDR, Linearity)

The linear dynamic range or linearity of the headspace is the relationship between the original concentrations (C_O) of analyte in the sample and its concentration in the headspace. The data variables used for quantitation of analytes are peak height. In section 2.5.4, the dynamic range was investigated by serial dilutions of a stock standard solution. Linear dynamic range is achieved when the coefficient of determination (R^2) is equal or greater than 0.99 (FDA, 2000). When the value of R^2 get closer to 1 (Miller and Miller, 2000) the slope of the regression line will provide the sensitivity of the regression and method to be validated. The linearity of DMA and TMA were determined in 2.8 for the laboratory-built thermal bath with GC-NPD system. The responses of DMA and TMA at various concentrations are shown in Tables 3.20-3.21 and Figures 3.24-3.25. For each concentration, five

replications were done and good precision was obtained since the relative standard deviations (RSD) were all lower than 4%. The HS-GC-NPD system showed a wide linear dynamic range, 2.7×10^{-3}-250 μg mL^{-1} for DMA and 0.30×10^{-3}-50 μg mL^{-1} for TMA, $R^2>0.99$.

Table 3.20 The responses of DMA at various concentrations

Concentration (μg mL^{-1})	Responses$\times10^6$ (μV)*
	DMA
0.5	0.007±0.001
1.0	0.018±0.001
5.0	0.236±0.004
7.5	0.240±0.002
10	0.29±0.01
25	2.2±0.02
50	6.0±0.1
75	8.2±0.3
100	11.0±0.3
150	17.2±0.2
175	20.1±0.6
200	21.9±0.3
225	24.4±0.5
250	27.5±0.4
275	27.6±1.0
300	28.5±0.7

*5 replications, RSD < 4 %

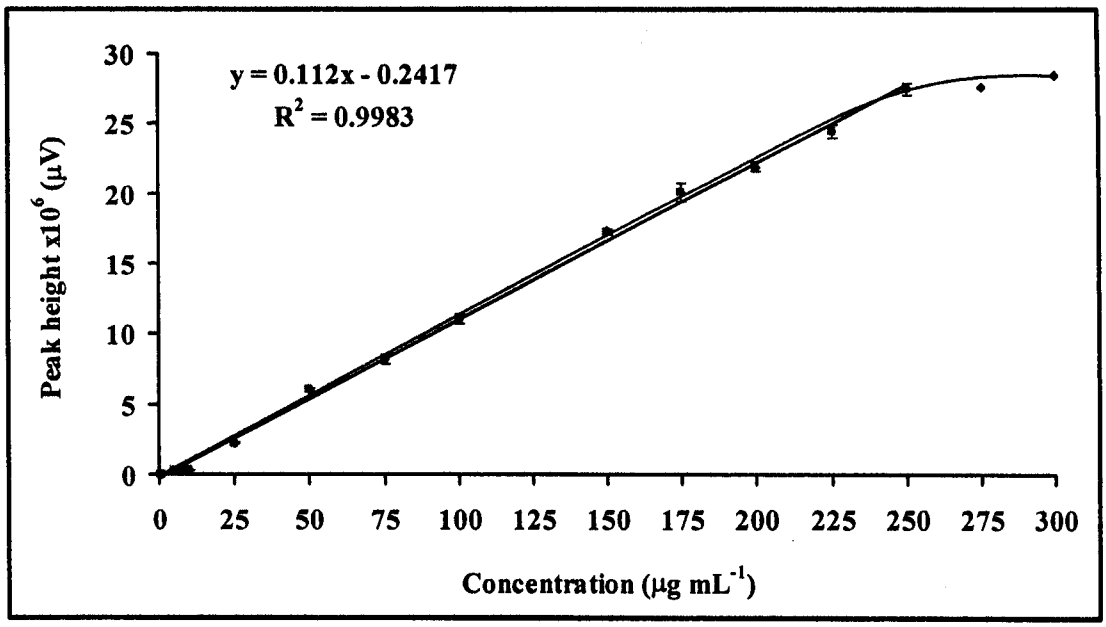

Figure 3.24 Linear dynamic range of DMA

Table 3.21 The responses of TMA at various concentrations

Concentration ($\mu g\ mL^{-1}$)	**Responses$\times 10^6$ (μV)* for TMA**
0.001	0.0040±0.0001
0.005	0.0029±0.0001
0.01	0.0089±0.0002
0.05	0.059±0.001
0.10	0.140±0.005
0.25	0.34±0.01
0.50	0.68±0.02
1.0	1.24±0.04
5.0	6.1±0.1
10	11.8±0.3
15	16.3±0.4
20	22.1±0.2
30	33.3±0.8
40	43.6±0.7
50	55.5±1.7
60	59.3±0.7
70	62.6±0.4
80	63.0±0.1

*5 replications, RSD < 4 %

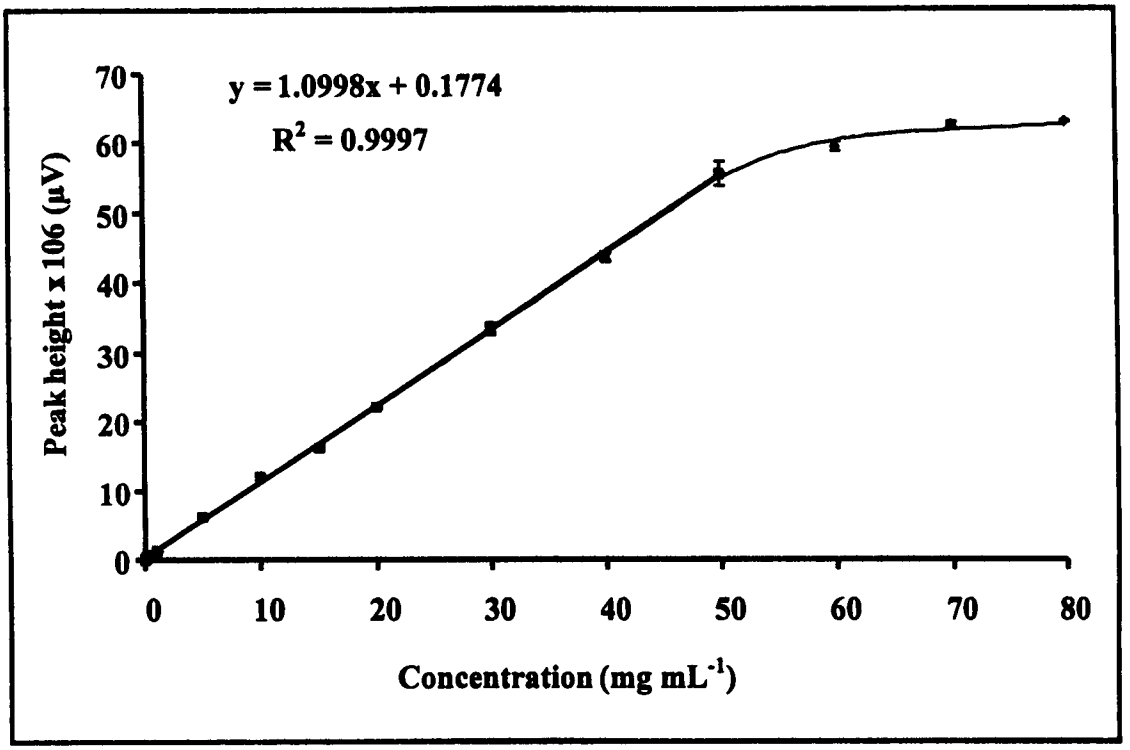

Figure 3.25 Linear dynamic range of TMA

3.3 Limit of detection (LOD)

The limit of detection (LOD) is the lowest concentration of an analyte in a sample that can be detected (Long and Winefordner, 1983). The limit of detection of DMA and TMA were investigated based on the IUPAC recommendation. The responses of blanks which appeared at retention times were measured. The maximum detectable blank signals are shown in Table 22 for headspace system. The limits of detection were calculated from equation 3.15, the standard calibration curves in Tables 3.20-3.21 and Figures 3.24-3.25.

$$C_L = \frac{kS_B}{m} \qquad (3.15)$$

Where C_L is the detectable concentration, k is the constant value at the confidence limit (k=3), S_B as the standard deviation of blank, for twenty repeatability and m is the slope of the calibration curve. The limits of detection of laboratory-built

system (HS-GC-NPD) were obtained for DMA and TMA 2.7 ng mL^{-1} and 0.30 ng mL^{-1} respectively as shown in Table 3.23.

Table 3.22 The data of the blank measurements by headspace technique, $n_B = 20$

t_R (min)	Maximum responses$\times 10^6$ (μV)*
1.28	0.21
1.28	0.20
1.28	0.21
1.29	0.20
1.28	0.20
1.29	0.22
1.29	0.20
1.29	0.19
1.30	0.21
1.29	0.20
1.29	0.21
1.29	0.20
1.29	0.22
1.29	0.21
1.29	0.21
1.29	0.22
1.29	0.19
1.29	0.21
1.28	0.21
1.29	0.19
$\overline{X}$	0.21
S_B	0.01

Table 3.23 The limit of detection for DMA and TMA standard solution with optimum conditions of HS-GC-NPD

Analytes	Limit of detection ($ng\ mL^{-1}$)
DMA	2.7
TMA	0.30

3.4 Sample Analysis

3.4.1 Sampling

Fish and shrimps were collected and analyzed by optimum conditions of HS-GC-NPD system. A total of 17 samples of fish and shrimp samples were sampling from local supermarkets and local fresh market in Hat Yai Songkhla as shown in Table 3.24.

Table 3.24 The information of samples

Type of samples	Variety of source	Number of sample
Indian mackerel	5	5
Sea bass	4	4
Giant tiger shrimp	2	2
White shrimp	6	6
Total samples	17	

3.4.2 Sample preparation

The ease of initial sample preparation is one of the advantages of static headspace extraction. Often, for qualitative analysis, the sample can be placed directly into the headspace vial and analyzed with no additional preparation. However for quantitation, it needs to use equilibrium system to obtain good sensitivity and accuracy for DMA and TMA, volatile organic compounds from solid samples. In this work, the matrices were fish and shrimp which were solid samples. Therefore, the physical state of the sample matrix needed to be changed. Two common approaches are crushing or grinding the sample and dissolving or dispersing the solid into a liquid. The first approach increases the surface area available for the volatile analyte to partition into the headspace. However, the analyte is still partitioning between a solid and the headspace. The second approach is preferred since liquid or solution sample matrices are generally easier to work than solid since the analyte partitioning process into the headspace usually reaches equilibrium faster. Also, analyte diffusion in liquids eliminates unusual diffusion path problems which often occur with solids and can unpredictably affect equilibration time (Mitra, 2003). For this work, fish and shrimp samples were ground and mixed with 3.33 mL ultra pure water into a 10 mL headspace vial and closed by septum and aluminium cap with climper and put the laboratory-built thermal bath before analysis at optimum conditions HS-GC-NPD system.

3.4.3 Sample size

For solid samples, diffusion takes much longer. This can be seen by comparing the order of magnitude of the diffusion coefficient, D: it order of magnitude is 10^{-6} in liquid and 10^{-8} to 10^{-11} in solids, while it is 10^{-1} in gases (Kolb and Ettre, 1997). Therefore, one characteristic of solid samples are the long equilibration times to increase the diffusion coefficient of DMA and TMA and enhance the analyte from liquid phase into gas phase (headspace), fish and shrimp samples were mixed in ultra pure water by adjustment the total sample volume at 3.33 mL (β=2). The results are shown in Table 3.25 and Figure 3.26. The sample size (fish

and shrimp tissue) at 1.5, 2.0 and 2.5 g gave nearly the same responses of DMA. When the sample size was lower than 1.5 g, it gave a lower response because of less analyte. For TMA, the sample size at 1.5 and 2.0 g gave nearly the same responses. The lower response at sample size 2.5 g could be because large amount of sample may reduce the diffusion coefficient in liquid phase. The sample size at 1.5 g was then selected as the optimum for sample analysis and validation method because it requires less sample.

Table 3.25 Effect of the sample size on the responses of DMA (25 μg mL^{-1}) and TMA (0.5 μg mL^{-1}) standard solutions

The amount of sample	**Responses×10^4 (μV)***	
	DMA	**TMA**
0.5	0.151±0.022	0.015±0.002
1.0	0.148±0.016	0.046±0.005
1.5	0.258±0.044	0.204±0.017
2.0	0.255±0.038	0.206±0.022
2.5	0.259±0.044	0.082±0.009

*5 replications, RSD < 17 %

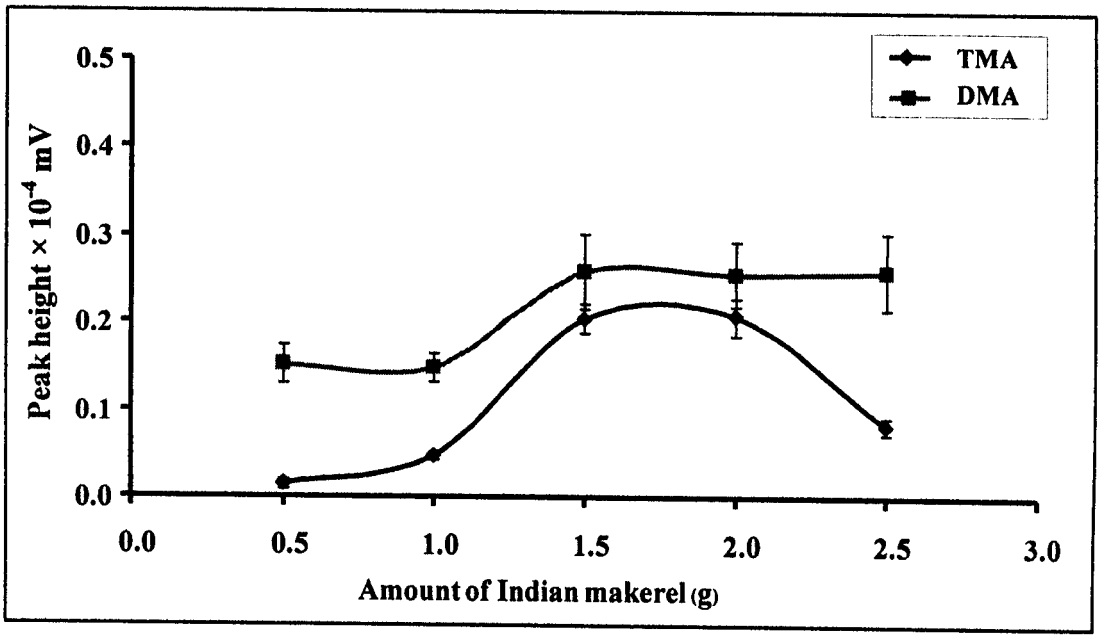

Figure 3.26 Responses of DMA (25 μg mL^{-1}) and TMA (0.5 μg mL^{-1}) standard solutions at various sample sizes

3.5 Matrix Interference

The various compositions in food could be interfered with the interest analyte in food analysis. If the analysts are not aware of this interference, it can lead to a number of different effects. One of the effects is enhancing the concentration of the analyte. Interference usually can affect the slope of the calibration curve and it could lead to a difference slope from the analyte of interest, so the slope of the calibration curve in the method of the standard additions may affect the linearity of the curve. This effect has the potential to indicate the possible present of hidden interferences (Eurachem guide, 1998). The matrix interference from two types of fish and two types of shrimp samples *i.e.*, Indian mackerel, Sea bass, Giant tiger shrimp and White shrimp were investigated. The matrix match calibration curve was used for this study by spiking various amounts of known standard of DMA and TMA into the sample as described in section 2.11. The optimum conditions were set for determining the spiking sample and standard DMA and TMA. If there is no matrix effect, the slope of standard curve and the spiked sample calibration should be equal (Eurachem,

1998). The results are shown in Tables 3.26-3.27 and Figures 3.27-3.28. When the standard and the spiked sample calibration curves were compared, both the DMA and TMA data did not give parallel regression lines and the slope of regression line in each group of standard curve and matrix match calibration curve were different.

Table 3.26 Effect of matrix on the responses of DMA in fish and shrimp samples

[DMA] ($\mu g\ mL^{-1}$)	Responses$\times 10^4$ (μV)* ± SD				
	Standard DMA	**Indian mackerel**	**Sea bass**	**Giant tiger shrimp**	**White shrimp**
25	2.28±0.06	0.48±0.01	0.17±0.01	0.37±0.04	0.19±0.01
50	4.65±0.16	1.42±0.04	1.02±0.18	1.12±0.11	1.20±0.03
100	11.63±0.33	3.16±0.02	3.24±0.46	3.92±0.50	2.97±0.05
150	17.10±0.59	5.0±0.2	6.02±0.63	5.61±0.63	5.60±0.03
200	22.38±0.73	6.97±0.08	8.93±1.33	8.71±0.97	7.47±0.09

*5 replications, RSD < 20 %

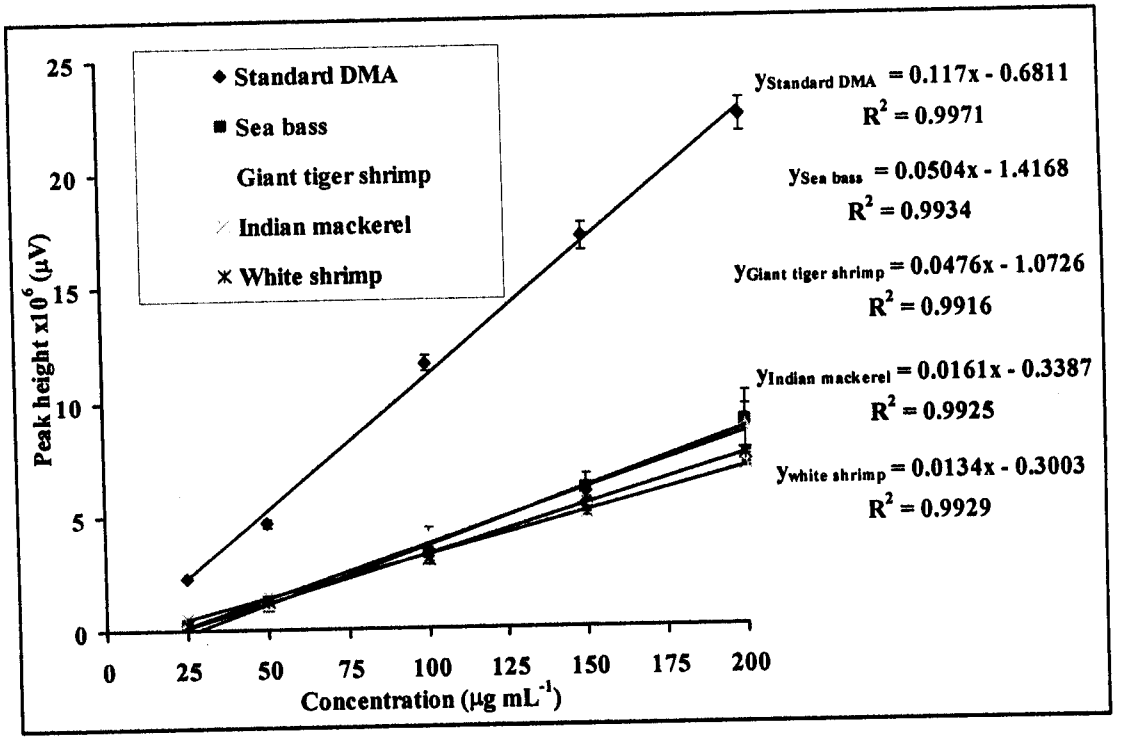

Figure 3.27 Matrix match calibration curves of DMA of fish and shrimp samples

Table 3.27 Effect of matrix on the responses of TMA in fish and shrimp samples

[TMA] (μg mL^{-1})	Responses×10^4 (μV)* ± SD				
	Standard TMA	Indian mackerel	Sea bass	Giant tiger shrimp	White shrimp
1	1.24±0.04	1.02±0.01	1.09 ±0.26	1.01±0.09	1.05±0.03
5	6.05±0.09	2.73±0.04	3.03±0.45	3.42±0.48	4.09±0.04
10	11.84±0.33	4.86±0.02	6.30±0.44	6.43±0.49	6.30±0.25
20	22.14±0.22	10.54±0.18	11.91±0.68	10.99±0.78	13.06±0.50
40	43.63±0.66	21.96±0.08	22.62±0.83	22.04±1.78	26.82±0.90

*5 replications, RSD < 20 %

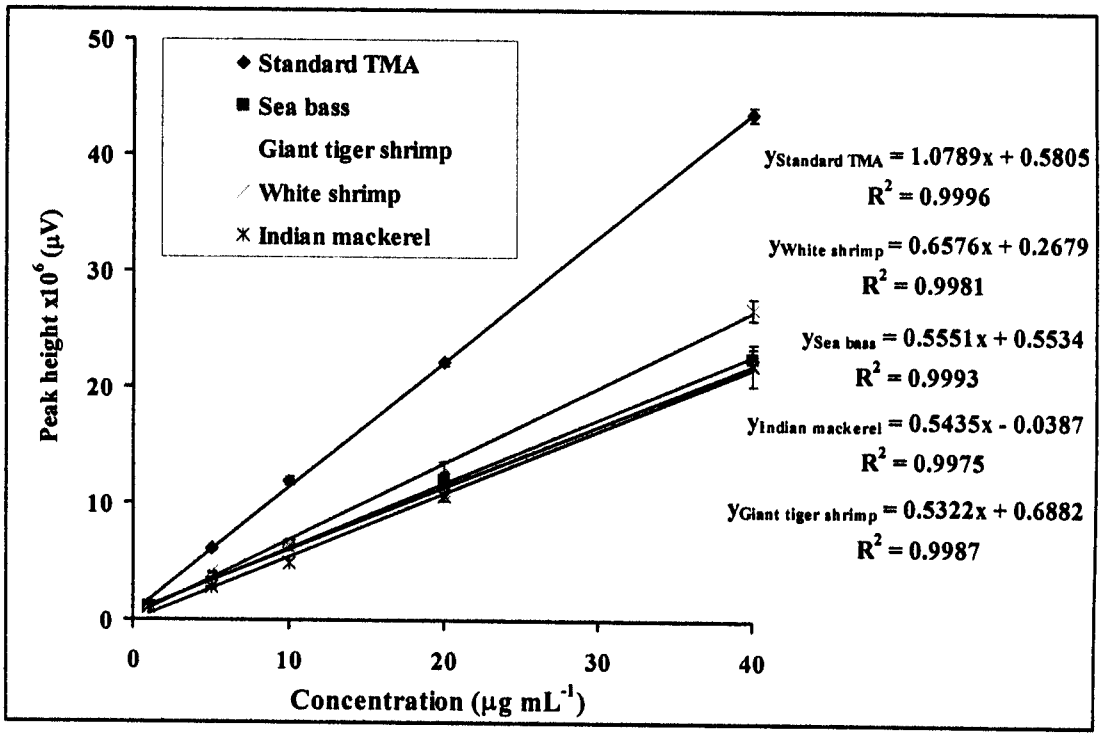

Figure 3.28 Matrix match calibration curves of TMA of fish and shrimp samples

The slopes of standard curve and matrix match calibration curves were tested using two-way analysis of variance (two-way ANOVA) by taking the null hypothesis (H_0) that the interaction of both slope is not significant and alternative hypothesis (H_1) that the interaction of slope is significant.

The results from significant test for comparison of the slopes of standard curve and matrix match calibration curves are shown in Tables 3.28-3.29. If *P* value is less than alpha (α, level of significance) then the null hypothesis was rejected at that significant level. From the results, it can be concluded that the slopes of regression line in standard curve and matrix match calibration curve were significant different as shown in Table 3.30. Therefore quantitative analysis of fish and shrimp samples must be determined from matrix match calibration curve (US-FDA, 2001).

Table 3.28 Statistic values for the comparison between the slope for DMA standard curve and matrix match calibration curve of various seafood samples

Matrix (type of seafood)	*Df*	Sum Sq	Mean Sq	*F*	*P*
Indian mackerel	4	332	83	1032	2.2×10^{-16}***
Sea bass	4	232	58	176	2.2×10^{-16}***
Giant tiger shrimp	4	252	63	290	2.2×10^{-16}***
White shrimp	4	290	72	937	2.2×10^{-16}***

Table 3.29 Statistic values for the comparison between the slope for TMA standard curve and matrix match calibration curve of various seafood samples

Matrix (type of seafood)	*Df*	Sum Sq	Mean Sq	*F*	*P*
Indian mackerel	4	701	175	2735	2.2×10^{-16}***
Sea bass	4	667	167	751	2.2×10^{-16}***
Giant tiger shrimp	4	726	182	374	2.2×10^{-16}***
White shrimp	4	435	109	632	2.2×10^{-16}***

Significant codes: '***' ($\alpha = 0.001$)

Where Df: Degree of freedom

Sum Sq: Sum square

Mean Sq: Mean square

F: ratio of two variances

P: Probability

Table 3.30 Level of significance (*P* value) from ANOVA for the comparison between the slope the standard curve and matrix match calibration curve of various seafood samples

Matrix	*P*	
	DMA	**TMA**
Indian mackerel	0.001	0.001
Sea bass	0.001	0.001
Giant tiger shrimp	0.001	0.001
White shrimp	0.001	0.001

3.6 Method validation

Method validation was performed to create the confidence in the analysis procedures. It provides an assurance of reliability during normal use (Swartz and Krull, 1997). To ensure the reliability of the results, method validation was evaluated by using standards, spiked samples, reagent and method blanks.

3.6.1 Accuracy and Recovery

Accuracy in HS-GC-NPD system was studied in term of recovery and precision (RSD). Recoveries of DMA and TMA in fish and shrimp samples were investigated by spiking known amount of DMA and TMA standard solution into fish and shrimp samples at concentration level of 100 and 200 μg mL^{-1} of DMA and 0.5 and 1 μg mL^{-1} of TMA (section 2.12.1). The responses obtained from spiked fish and shrimp samples for the mixture of DMA and TMA standard solution were compared. Recoveries were 54-69% for DMA (0.5 and 1 μg mL^{-1}) and 53-70% for TMA (0.5 and 1 μg mL^{-1}) (Tables 3.31 and 3.32). For DMA and TMA there are no regulation for recovery but these values of recovery are acceptable by EPA method 8070A in 1996 (13-109% recovery) for the analysis of nitrosamines by gas chromatographic

method in solid matrices which are similar to DMA and TMA. The recovery in this study is better than obtained by other works of HS-GC technique *i.e.*, the determination of volatile organochlorine compounds in landfill leachate and treated leachate which reported the recoveries in range of 24.7 to 26.9% for landfill leachate and 25.3 to 26.0% of treated leachate (Flórez Menéndez *et al.*, 2004) and volatile organic compounds in sediment samples which reported the recoveries in range of 6.5-97.6% (Kawata *et al.*, 1997). The recovery, SD and %RSD for the fortified fish and shrimp samples indicated in Tables 3.31 and 3.32. The RSDs ranged from 3.8-11.8% (%RSD, recommend method ±20).

Table 3.31 Recovery of DMA of various fish and shrimp samples at spiked concentrations of 100 and 200 μg mL^{-1}

Type of samples	**Recovery* (%) ± SD**	
	100 μg mL^{-1}	**200 μg mL^{-1}**
Indian mackerel	65±6	68±3
Sea bass	60±5	59±5
Giant tiger shrimp	61±4	54±6
White shrimp	60±2	69±4

*5 replications, RSD < 11.5 %

Table 3.32 Recovery of TMA of various fish and shrimp samples at spiked concentrations of 0.5 and 1 μg mL^{-1}

Type of samples	Recovery* (%) ± SD	
	0.5 μg mL^{-1}	1 μg mL^{-1}
Indian mackerel	63±6	53±6
Sea bass	67±6	59±4
Giant tiger shrimp	68±4	62±5
White shrimp	70±8	56±4

*5 replications, RSD < 11.8 %

3.6.2 Precision

The precision is the measure of the degree of repeatability of an analytical method as the percent relative standard deviation for a statistically significant number of samples (Swartz and Krull, 1997). Repeatability is a type of precision relating to measurements made under repeatable conditions *i.e.*, same method, same material, same operator and same laboratory (Eurachem, 2002). In this study, two types of fish and two types of shrimp samples were evaluated at two spiking level of 100 and 200 μg mL^{-1} for DMA, and 0.5 and 1 μg mL^{-1} for TMA, respectively, in each fish and shrimp samples followed by headspace technique before analysis in section 2.5.4. Five replicate analyses were performed at each concentration. The results are shown in Tables 3.33 and 3.34 their relative standard deviations (RSD) were 3.8-11.8%, lower than 20% (EPA, 8021B), the maximum %RSD that is allowed at spiked concentration 100 and 200 μg mL^{-1} for DMA and 0.5 and 1 μg mL^{-1} for TMA.

Table 3.33 Precision of DMA of various fish and shrimp samples at spiked concentrations of 100 and 200 μg mL^{-1}

Type of samples	Precision*, RSD (%)	
	100 μg mL^{-1}	200 μg mL^{-1}
Indian mackerel	9.6	4.7
Sea bass	8.6	8.5
Giant tiger shrimp	6.3	11.5
White shrimp	3.8	6.4

*5 replications, RSD < 11.5 %

Table 3.34 Precision of TMA of various fish and shrimp samples at spiked concentrations of 0.5 and 1 μg mL^{-1}

Type of samples	Precision*, RSD (%)	
	0.5 μg mL^{-1}	1 μg mL^{-1}
Indian mackerel	9.7	11.8
Sea bass	9.5	8.3
Giant tiger shrimp	6.3	7.3
White shrimp	10.9	8.0

*5 replications, RSD < 11.8 %

3.7 Qualitative and quantitative analysis of DMA and TMA in fish and shrimp samples

3.7.1 Qualitative Analysis

The optimum conditions of HS-GC-NPD were used to analyze DMA and TMA in fish and shrimp samples. For qualitative analysis, the retention time, t_R, of the sample chromatogram was compared with retention time of the standard

chromatogram to identify the DMA and TMA peak. The average t_R of DMA was 1.43±0.01 minutes and TMA was 1.28±0.01 minutes.

3.7.2 Quantitative Analysis

Quantitative analysis of DMA and TMA were done by considering the responses *i.e.*, peak height that was related to concentration of the analytes. Two types of fish and two types of shrimp samples *i.e.*, Indian mackerel, Sea bass, Giant tiger shrimp and White shrimp were sampling from local fresh markets and local supermarkets. All samples were prepared and analyzed at the optimum conditions in 2.5.4. The samples were analyzed by HS-GC-NPD using optimum conditions and representative chromatogram of the two types of fish and two types of shrimp samples are shown in Figure 3.29. The DMA in fish and shrimp samples were obtained in the range 2.17-5.15 and 2.35-4.55 mg/100g, respectively as shown in Table 3.35. TMA in fish and shrimp samples were obtained in the range 0.11-7.69 and ND-5.22 mg/100g, respectively (Table 3.36).

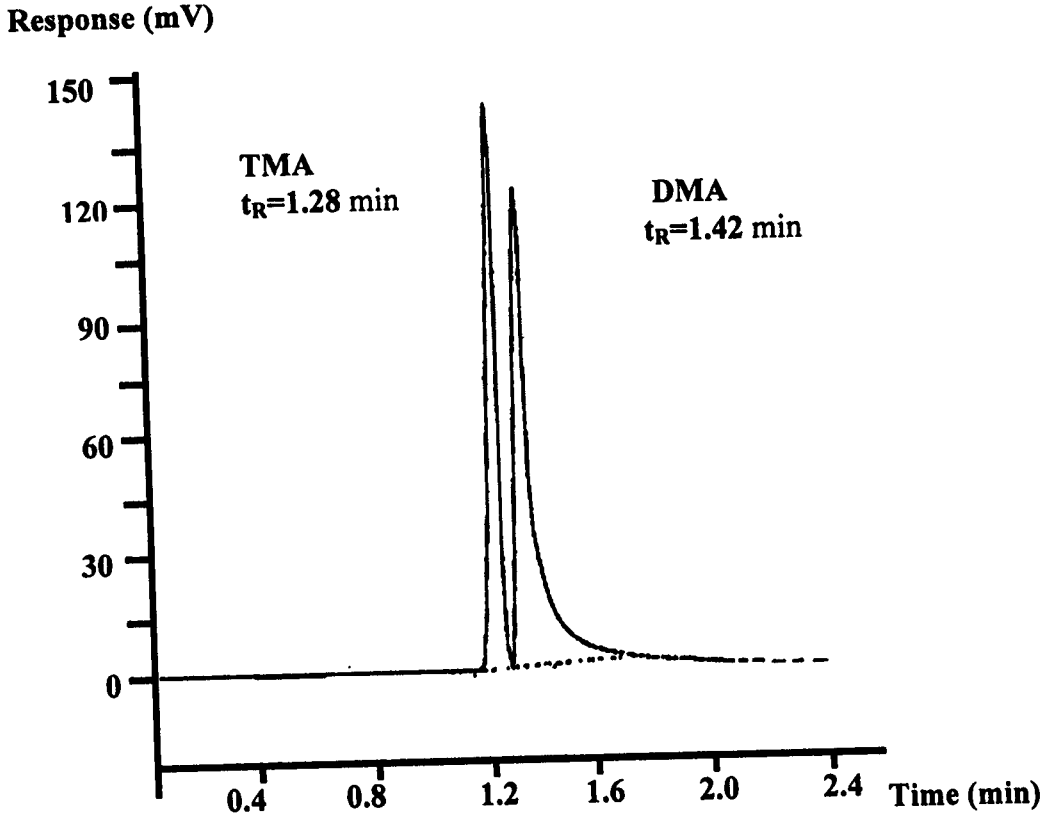

Figure 3.29 HS-GC-NPD Chromatogram of DMA and TMA from spiked Indian mackerel fish sample

Table 3.35 Amount of DMA in fish and shrimp samples by matrix match calibration curve

Sources	Amount of DMA (mg/100g)			
	Indian mackerel	**Sea bass**	**Giant tiger shrimp**	**White shrimp**
S1	5.15±0.08	4.63±0.13	2.67±0.05	4.55±0.11
S2	4.65±0.29	3.07±0.02	NS	2.51±0.04
S3	2.48±0.02	3.01±0.01	2.36±0.01	3.12±0.01
S4	2.28±0.02	NS	NS	2.54±0.03
S5	2.17±0.01	NS	NS	2.35±0.01
S6	NS	3.01±0.01	NS	3.12±0.01

ND= Not Detectable

NS= Not Sampling

S1= Klongrean fresh market

S2= Carrefour

S3= Natural fresh market

S4= Plaza market

S5= Samchai fresh market

S6= Tesco Lotus

Table 3.36 Amount of TMA in fish and shrimp samples by matrix match calibration curve

Sources	Amount of TMA (mg/100g)			
	Indian mackerel	**Sea bass**	**Giant tiger shrimp**	**White shrimp**
S1	4.65±0.11	3.27±0.10	1.12±0.09	1.85±0.14
S2	7.69±0.13	1.96±0.04	NS	ND
S3	1.05±0.27	0.11±0.02	0.69±0.02	5.22±0.22
S4	0.72±0.11	NS	NS	3.10±0.30
S5	1.77±0.17	NS	NS	ND
S6	NS	4.94±0.02	NS	ND

ND= Not Detectable

NS= Not Sampling

S1= Klongrean Fresh market

S2= Carrefour

S3= Natural Fresh market

S4= Plaza market

S5= Samchai Fresh market

S6= Tesco Lotus

3.7.3 The criteria for quality of fish product

Freshness is one of the most important criteria for quality of fish product. However, fish undergoes irreversible change (colour, texture and smell) after harvest, resulting in quality loss (Timm and Jørgensen, 2002). DMA and TMA have often been used to be an index of spoilage (Krzymien and Elias, 1990). For TMA, the EU acceptable quality and safety limits are set at 12 mg per 100 g (The European Commission Council Regulation No. 91/493/EEC, 1991). For DMA, although there is no specific limit but it can react with nitrile compounds to form a nitroso-dimethylamine (carcinogen compound). From the real sample analysis of both fishes and shrimps in the local market the values obtained are quite low *i.e.*, they are fresh and safe.